Bioconjugate Chemistry

pubs.acs.org/bc Article

DiPODS: A Reagent for Site-Specific Bioconjugation via the Irreversible Rebridging of Disulfide Linkages

Elaheh Khozeimeh Sarbisheh,[#] Guillaume Dewaele-Le Roi,[#] Whitney E. Shannon, Sally Tan, Yujia Xu, Brian M. Zeglis,* and Eric W. Price*

Cite This: *Bioconjugate Chem.* 2020, 31, 2789−2806 Read Online

ACCESS | Metrics & More | Article Recommendations | Supporting Information

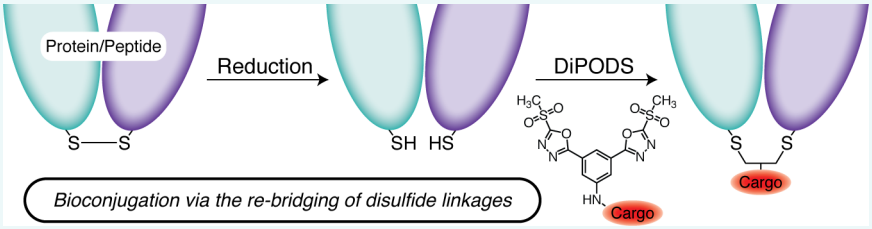

ABSTRACT: Chemoselective reactions with thiols have long held promise for the site-specific bioconjugation of antibodies and antibody fragments. Yet bifunctional probes bearing monovalent maleimides—long the "gold standard" for thiol-based ligations—are hampered by two intrinsic issues: the *in vivo* instability of the maleimide−thiol bond and the need to permanently disrupt disulfide linkages in order to facilitate bioconjugation. Herein, we present the synthesis, characterization, and validation of DiPODS, a novel bioconjugation reagent containing a pair of oxadiazolyl methyl sulfone moieties capable of irreversibly forming covalent bonds with two thiolate groups while simultaneously rebridging disulfide linkages. The reagent was synthesized from commercially available starting materials in 8 steps, during which rotamers were encountered and investigated both experimentally and computationally. DiPODS is designed to be modular and can thus be conjugated to any payload through a pendant terminal primary amine (DiPODS−PEG_4−NH_2). Subsequently, the modification of a HER2-targeting Fab with a fluorescein-conjugated variant of DiPODS (DiPODS−PEG_4−FITC) reinforced the site-specificity of the reagent, illustrated its ability to rebridge disulfide linkages, and produced an immunoconjugate with *in vitro* properties superior to those of an analogous construct created using traditional stochastic bioconjugation techniques. Ultimately, we believe that this work has particularly important implications for the synthesis of immunoconjugates, specifically for ensuring that the attachment of cargoes to immunoglobulins is robust, irreversible, and biologically and structurally benign.

INTRODUCTION

Over the last two decades, immunoconjugates have emerged as vitally important therapeutic and diagnostic tools. However, the imprecise synthetic methods used to create many antibody−drug conjugates (ADCs) and radioimmunoconjugates remains an impediment to their widespread success.[2] Traditional approaches to bioconjugation are predicated on the indiscriminate attachment of payloads—e.g., chelators, fluorophores, or toxins—to lysine residues within antibodies. Yet these non-site-specific synthetic strategies inevitably lead to heterogeneous product mixtures and can produce constructs with suboptimal immunoreactivity and *in vivo* performance.

In light of these issues, the development of "site-specific" bioconjugation methods designed to append cargoes *only* at well-defined sites within an antibody's macromolecular structure has become an area of intensive research.[3−8] A wide variety of these approaches have been devised, including variants based on the manipulation of the heavy chain glycans, the use of peptide tags, and the genetic incorporation of unnatural amino acids. Far and away the most popular methods, however, rely upon the reaction between maleimide-based bifunctional probes and cysteine residues within the biomolecule (Figure 1A). While maleimide-based bioconjugation strategies are undeniably facile, rapid, and modular, they nonetheless suffer from a critical flaw: the inherent instability of the thioether bond between the maleimide and the cysteine. The Michael addition reaction that forms this linkage is reversible *in vivo* both spontaneously (retro-Michael) and in the presence of competing thiols.[9,10] This, of course, can be a significant problem. In the context of radioimmunoconjugates, for example, this process can result in the *in vivo* release of radionuclides, reducing target-to-background activity concen-

Received: October 30, 2020
Revised: November 6, 2020
Published: November 19, 2020

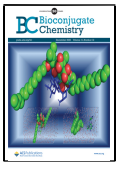

https://dx.doi.org/10.1021/acs.bioconjchem.0c00590
Bioconjugate Chem. 2020, 31, 2789−2806

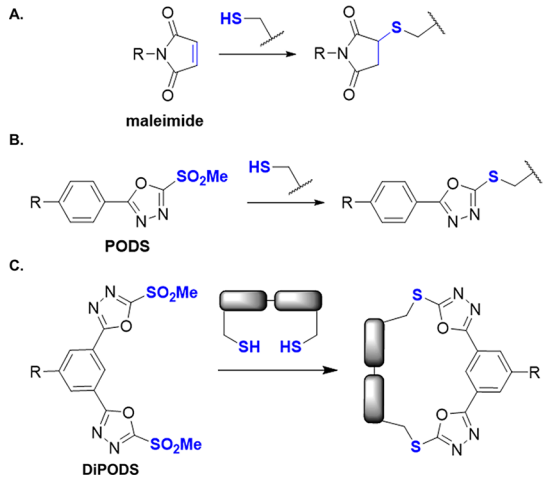

Figure 1. Schematics of thiol-based bioconjugations using (A) maleimide-, (B) PODS-, and (C) DiPODS-based bifunctional reagents.

tration ratios and increasing radiation doses to healthy tissues.[11−15]

Two years ago, in an effort to circumvent the inherent limitations of maleimides, we reported the synthesis, characterization, and *in vivo* validation of an alternative: PODS.[3] Inspired by the work of the late Carlos Barbas III, PODS is an easily synthesized phenyloxadiazolyl methyl sulfone-based reagent capable of rapidly and irreversibly forming covalent linkages with thiols (Figure 1B).[16−19] This work clearly illustrated that a ^{89}Zr-DFO-labeled variant of the huA33 antibody synthesized using a PODS-based bifunctional chelator exhibited superior *in vitro* stability and—even more importantly—*in vivo* performance compared to an analogous radioimmunoconjugate synthesized using a traditional, maleimide-based probe.[3] Furthermore, the innate modularity of PODS enabled the creation of PODS-CHX-A″-DTPA and PODS-DOTA bifunctional chelators for the synthesis of radioimmunoconjugates labeled with lutetium-177 and actinium-225.

While PODS-based reagents represent a distinct improvement compared to their maleimide-based forerunners, neither tool can avoid an intrinsic problem common to the overwhelming majority of thiol-targeted bioconjugations. In the absence of free cysteine residues incorporated via genetic engineering, all of the cysteines within an antibody are paired to form 8 intrachain and 8 interchain disulfide bridges. As a result, thiol-based bioconjugation strategies require the reduction of these disulfide bridges to generate free thiols, with the slightly easier-to-reduce interchain linkages often the target of selective scission.[8] While the subsequent reaction of these free cysteines with thiol-selective probes enables the site-specific attachment of cargoes to the immunoglobulin, it simultaneously seals the fate of the broken disulfide bridges, potentially reducing the stability of the macromolecule and attenuating effector functions.[20] A handful of reagents capable of reacting with *two* thiols and thus reforming the covalent bridge between the reduced cysteine residues have been developed.[20−33] However, immunoconjugates synthesized using the most widely studied of these tools—dibromo- and dithiophenolmaleimides—are still prone to instability *in vivo*. While the developers of this "next generation maleimide" technology tout this reversibility as an advantage in the context of ADCs, it nonetheless remains an obstacle for radioimmunoconjugates.

Herein, we present the development and evaluation of **DiPODS**, a novel reagent bearing *two* oxadiazolyl methyl sulfone moieties designed to provide a modular platform for irreversible bioconjugations while simultaneously rebridging disulfide linkages (Figure 1C). Following the synthesis and chemical characterization of the DiPODS scaffold—during which rotamers were discovered and investigated both experimentally and computationally—a fluorescein-labeled variant of the reagent (DiPODS-FITC) was created for proof-of-concept bioconjugation experiments. More specifically, the reaction conditions for DiPODS-FITC were optimized using both isotype-control and HER2-targeting Fab fragments, and the FITC-bearing immunoconjugates were characterized via gel electrophoresis, size exclusion HPLC, and circular dichroism spectroscopy. Finally, the cell binding behavior of the HER2-targeting Fab-DiPODS-FITC was interrogated via flow cytometry and compared to that of an analogous Fab-FITC immunoconjugate created via a traditional, stochastic lysine-based approach to bioconjugation.

RESULTS AND DISCUSSION

Synthesis and Characterization. DiPODS was prepared in 8 synthetic steps with good to high yield at each step, but the synthetic journey was tortuous (Scheme 1). The synthesis began with the Boc-protection of aminoisophthalate, which followed a published procedure with some minor alteration.[34] The Boc-protection was performed under nitrogen atmosphere overnight and produced compound **1** with 74% yield after purification. Surprisingly, the ^{1}H NMR spectrum of the crude mixture of compound **1** revealed three sets of signals for all

Scheme 1. Optimized Synthesis of DiPODS in 8 Steps for a Cumulative Yield of ∼15%

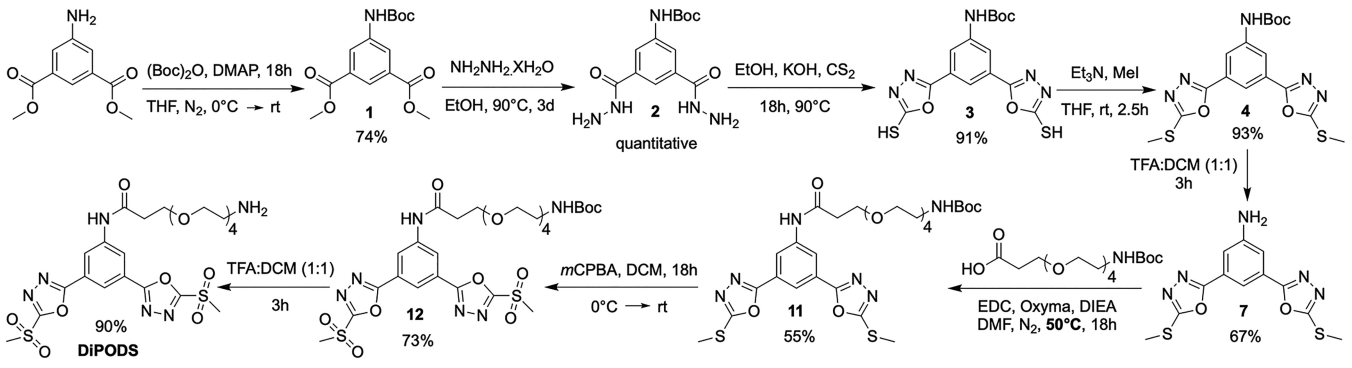

https://dx.doi.org/10.1021/acs.bioconjchem.0c00590
Bioconjugate Chem. 2020, 31, 2789−2806

Scheme 2. Attempted Reaction Schemes in Pursuit of DiPODS[a]

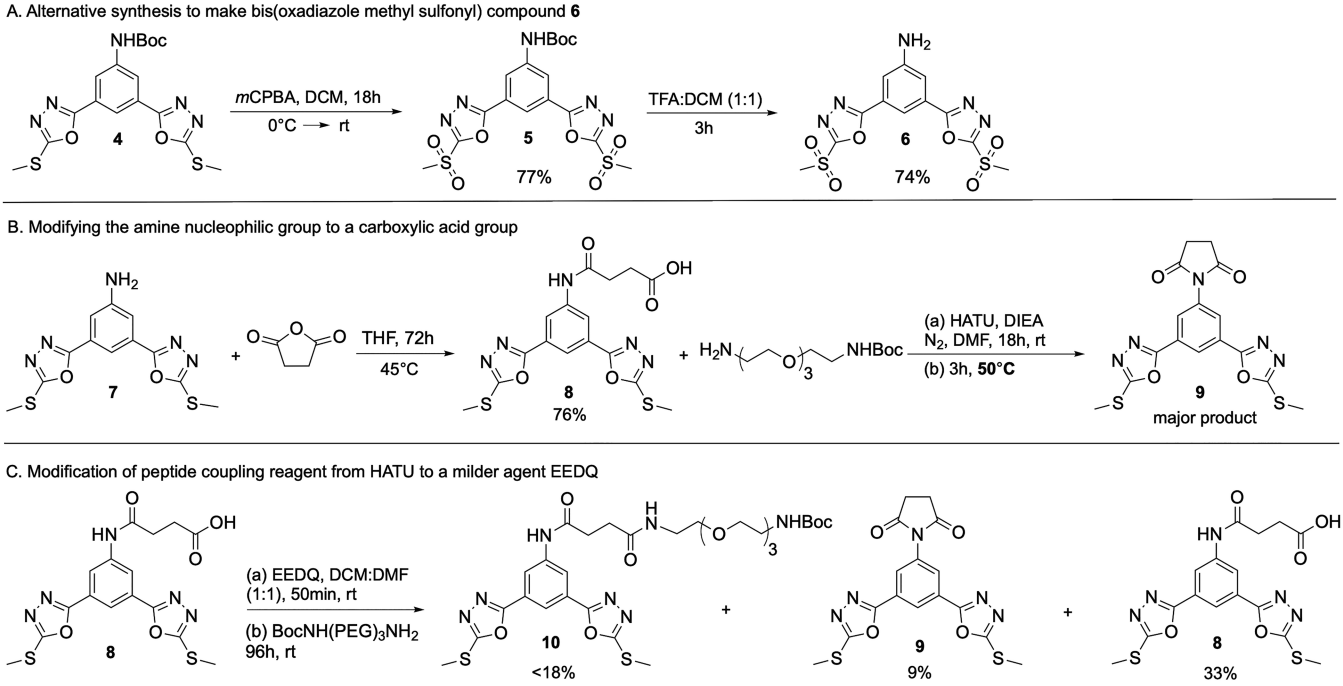

[a](A) Synthesis of the ultimately unreactive compound **6**; (B) modification of the weakly nucleophilic aryl-amine **7** to form carboxylic acid-bearing **8** and, subsequently, "dead end" compound **9**; (C) peptide coupling of compound **8** to produce the desired product, compound **10**, in <18% yield.

functional groups except for the proton of the secondary amine, which was represented by a single broad peak in the ^{1}H NMR spectra (*vide infra*). While a combination of normal-phase chromatography and precipitation facilitated the partial separation of these products, all three revealed the same molecular weight by mass spectrometry, suggesting that they are conformers of **1** (for further exploration of this phenomenon, see below). The crude mixture of **1** was then treated with hydrazine hydrate and, somewhat surprisingly, produced 5-amino isophthalic dihydrazide **2** in quantitative yield. This intermediate was subsequently treated with ethanol, KOH, and carbon disulfide to create phenyl-bis(oxadiazole thiol) **3** in 91% yield. Next, the methylation of **3** using methyl iodide generated the bis(methyl thioether) **4** in near-quantitative yield.

The first challenges in the synthesis emerged as we progressed beyond compound **4**. In our first attempt, bis(methyl thioether) **4** was directly oxidized via *meta*-chloroperoxybenzoic acid (*m*CPBA) to form the bis(methyl sulfonyl) **5** followed by Boc-deprotection to form compound **6** (Scheme 2A). The plan was to use compound **6** in a coupling reaction with a carboxylic acid-bearing poly(ethylene glycol) (PEG) chain. However, several attempts at this peptide coupling reaction failed or resulted in unacceptably poor yields. Aryl amine groups are notoriously poor nucleophiles, and we believe that the reactivity of the aryl-amine in compound **6** is reduced even further by the electron-withdrawing methyl sulfonyl substituents.

Methyl thioether groups are less electron-withdrawing than the methyl sulfonyl substituents. Following this logic, we decided to perform the coupling reaction prior to the formation of the methyl sulfonyl moieties with the hope that this version of the aryl-amine had enhanced nucleophilicity. To this end, compound **4** was first deprotected in quantitative yield to produce **7**. Subsequently, in the first attempt at coupling, 1-[bis(dimethylamino)methylene]-1*H*-1,2,3-triazolo-[4,5*b*]pyridinium 3-oxide (HATU) was used alongside *N*,*N*-diisopropylethylamine (DIEA). These conditions yielded <15% of the desired product, a result that mass spectrometry analysis suggested is related to the degradation of the starting materials. In response, DIEA was then swapped for a milder base—2,4,6-trimethylpyridine (TMP)—and the reaction was attempted at room temperature as well as 50 °C, yet both attempts proved unsuccessful. Next, we decided to change our synthetic strategy and reverse the coupling chemistry by transforming the aryl-amine into a carboxylic acid via the reaction of **7** with succinic anhydride to form **8** (Scheme 2B).

With compound **8** now containing a carboxylic acid, we attempted a peptide coupling reaction with a mono-Boc-protected bisamino-PEG chain, but the use of HATU and DIEA at both room temperature and 50 °C resulted in an unwanted cyclization and the formation of compound **9**—a clear dead end—as the major product. This same transformation was then attempted using *N*-ethoxycarbonyl-2-ethoxy-1,2-dihydroquinoline (EEDQ) as an alternative coupling reagent (Scheme 3C). Disappointingly, this reaction resulted in the recovery of nearly 33% starting material as well as two products: the cyclized phenyl succinimide **9** (9% yield) and the desired product **10** (<18% yield).

To continue our efforts to search for a higher yielding route forward, we returned to bis(methyl thioether) **7** as a starting point to test a new set of peptide coupling conditions: oxyma with 1-ethyl-3-(3-(dimethylamino)propyl)carbodiimide (EDC) (Scheme 1). At room temperature, this reaction yielded <10% of the desired product (compound **11**), with mass spectrometry revealing the presence of unreacted starting material **7** as well as the *O*-acylisourea-activated EDC intermediate. Suspecting that the EDC intermediate was

https://dx.doi.org/10.1021/acs.bioconjchem.0c00590
Bioconjugate Chem. 2020, 31, 2789−2806

Scheme 3. Synthesis of DiPODS−PEG$_4$−FITC (DiPODS-FITC)

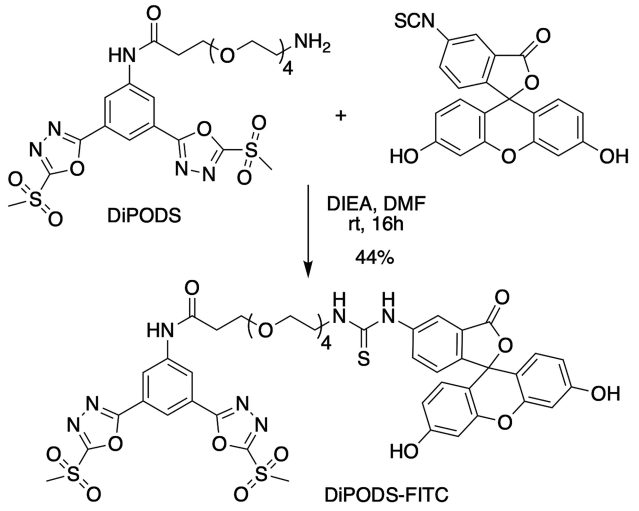

trapped in a step with an energy barrier that was impassable at room temperature, we repeated the same reaction at 50 °C. This time, the PEGylated product **11** was obtained in 55% yield. To complete the sequence, **11** was then oxidized with *m*CPBA to create bis(methylsulfonyl) **12** in 73% yield, and—finally—compound **12** was deprotected to provide DiPODS (DiPODS-PEG$_4$-NH$_2$) in ∼90% yield. We concluded this synthetic journey with an 8-step synthetic route to produce DiPODS with a cumulative yield of ∼15%. As synthesized, DiPODS is modular and can be coupled to any number of different bifunctional chelators, dyes, or other payloads. The primary amine of DiPODS can be reacted with a number of electrophilic bioconjugation reagents such as activated esters or phenyl-isothiocyanates.

Variable Temperature NMR. Before interrogating the reactivity of DiPODS, we thought it interesting and important to take a more detailed look at the intriguing structural data collected for compound **1**. As we noted above, the ^{1}H NMR of the crude mixture of **1** revealed a mixture presumed to be composed of conformers (Figure 2A and B). The ^{1}H NMR spectrum contained three sets of signals—sets **A**, **B**, and **C**—for each functional group, with the exception of the Boc-protected amine, which produced a single broad peak (Figure 2B, Figure S1). Curiously, the use of this mixture—without any separation—resulted in the formation of compound **2** in quantitative yield (Scheme 1).

In an attempt to separate and identify the components of the crude product mixture, it was dissolved in warm DCM and stored at −20 °C overnight. The first attempt at precipitation produced a shiny white precipitate that was separated from the mother liquor via filtration and dried under high vacuum. The ^{1}H NMR of this white precipitate displayed only one set of signals—set **A**—for all the functional groups, including the proton of the secondary amine (Figures 2C and S8). The isolation of pure set **A**, and the following investigation of the remaining mother liquor mixture by VT-NMR strongly suggests that compound **1**—like many other carbamate-bearing molecules—exists as *syn*- and *anti*-rotamers.[35,36] The *anti*-rotamers of compound **1** are more energetically favored

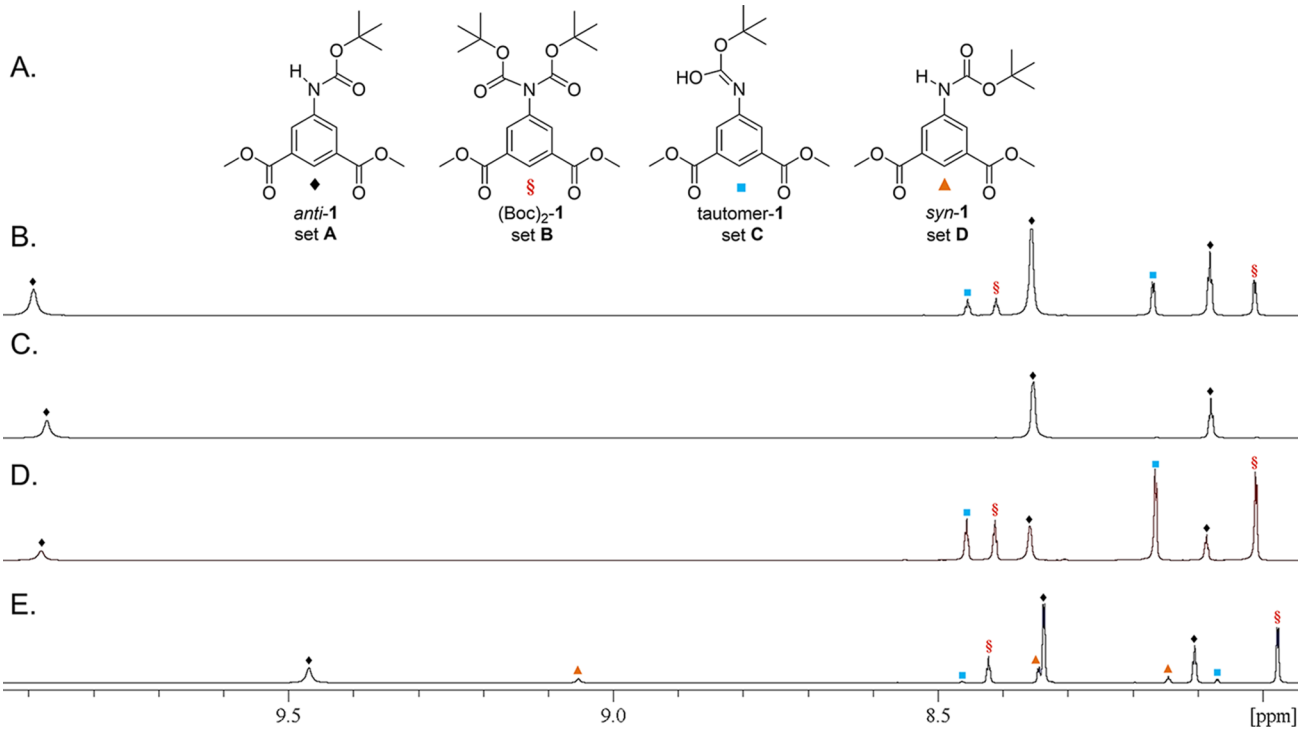

Figure 2. (A) Structures of each component discovered in the compound **1** mixture, as well as the corresponding ^{1}H NMR spectra in [D$_6$]DMSO of the aromatic region of (B) the crude mixture before precipitation or column chromatography, (C) the isolated precipitate from cold DCM, (D) the final mother liquor containing a mixture of all 3 components at 25 °C, and (E) the final mother liquor mixture at 90 °C. Peaks associated with the *anti* rotamers of compound **1** (*anti*-**1**, set **A**, ♦), a doubly Boc-protected derivative of compound **1** [(Boc)$_2$-**1**, set **B**, red §], an imidic acid tautomer of compound **1** (tautomer-**1**, set **C**, blue ■), and the *syn* rotamers of compound **1** (*syn*-**1**, set **D**, brown ▲) are designated by the symbols ♦, red §, blue ■, and brown ▲, respectively. For simplicity, only one conformer of each species is shown in the inset.

https://dx.doi.org/10.1021/acs.bioconjchem.0c00590
Bioconjugate Chem. 2020, 31, 2789−2806

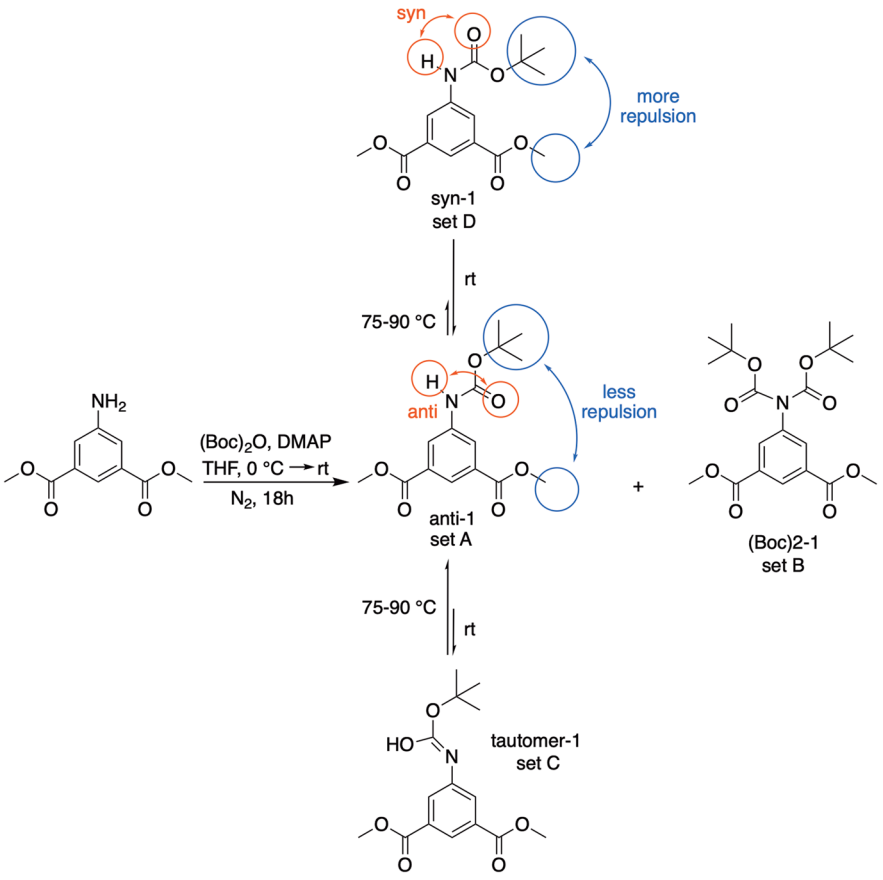

Figure 3. Product mixture of compound **1**. Only one conformer of each species is shown.

due to less steric hindrance between the *tert*-butyl group and the ester group (Figures 2A and 3; for a more detailed discussion, see Computational Studies). Therefore, the signals of set **A** were assigned to a mixture of the *anti*-rotamer of compound **1**. To be more specific, while the *anti*-rotamer configuration of the Boc group remains constant, the two methyl ester groups can rotate freely, creating a subset of conformers for each of the *syn*- and *anti*-rotamers (i.e., subconformers).

After isolating the precipitate from the crude product mixture, the solvent was removed from the mother liquor, and the solid residue was subjected to several more rounds of precipitation. After each round, the precipitate was isolated, and each time it was found via ^{1}H NMR to be predominantly composed of the *anti* -rotamer (set **A**). Following several rounds of precipitation, the aggregate mother liquor was concentrated under vacuum and found via ^{1}H NMR to contain both sets **B** and **C** as well as a small amount of set **A** (Figures S31 and 2D). In order to better understand the NMR spectrum of the product mixture of compound **1**, a series of NMR spectra were collected at different temperatures. Two NMR samples were prepared from the components of crude compound **1**. The first contained only the precipitate, i.e., the *anti*-rotamers (Figure 2C, set **A**). The second contained the mixture isolated from the mother liquor following precipitation (Figure 2D). The latter is composed mostly of the compounds responsible for sets **B** and **C** but also some of the *anti*-rotamer (set **A**). A more detailed explanation of the VT-NMR experiments and assignments can be found in the Materials and Methods and the Supporting Information (Figures S36 and S37), with the results summarized in Figures 2 and 3.

Ultimately, set **B** was attributed to a doubly Boc-protected version of compound **1** based on the integration ratio between the methyl ester (6) and *tert*-butyl (18) protons, as well as the presence of a tertiary amine group with no proton signal. High resolution mass spectrometry subsequently confirmed this assignment. As removing the first of two Boc protecting groups is easier than the second, the doubly protected compound (set **B**) appears to be converted to compound **1** at elevated temperatures (VT NMR, Figure 2E, Table S1, and Figures S36 and S37). Set **C**, in contrast, has an integration ratio of 6:9 between the methyl ester (6) and *tert*-butyl (9) protons, confirming that the compound responsible for these peaks has a single Boc group. However, no proton associated with the amine was observed. Furthermore, upon heating to 90 °C set **C** disappeared almost entirely. We propose that this phenomenon can be explained by a tautomerization reaction involving the transfer of a proton from the amine to the neighboring oxygen (Figure 3). The assignment of set **C** as a tautomeric form of set **A** would explain why the integration of the former matches that of the latter except for the absence of the proton from the amine group. In the end, these NMR data permit us to deconvolute the constituents of the original compound **1** product mixture: an *anti*-rotamer of compound **1** (*anti*-**1**, set **A**), a doubly Boc-protected variant of compound **1** [(Boc)$_2$-**1**, set **B**], and an imidic acid tautomer of compound **1** (tatomer-**1**, set **C**) (Figure 3). These findings also explain how a crude mixture of **1** containing all of these components was

https://dx.doi.org/10.1021/acs.bioconjchem.0c00590
Bioconjugate Chem. 2020, 31, 2789−2806

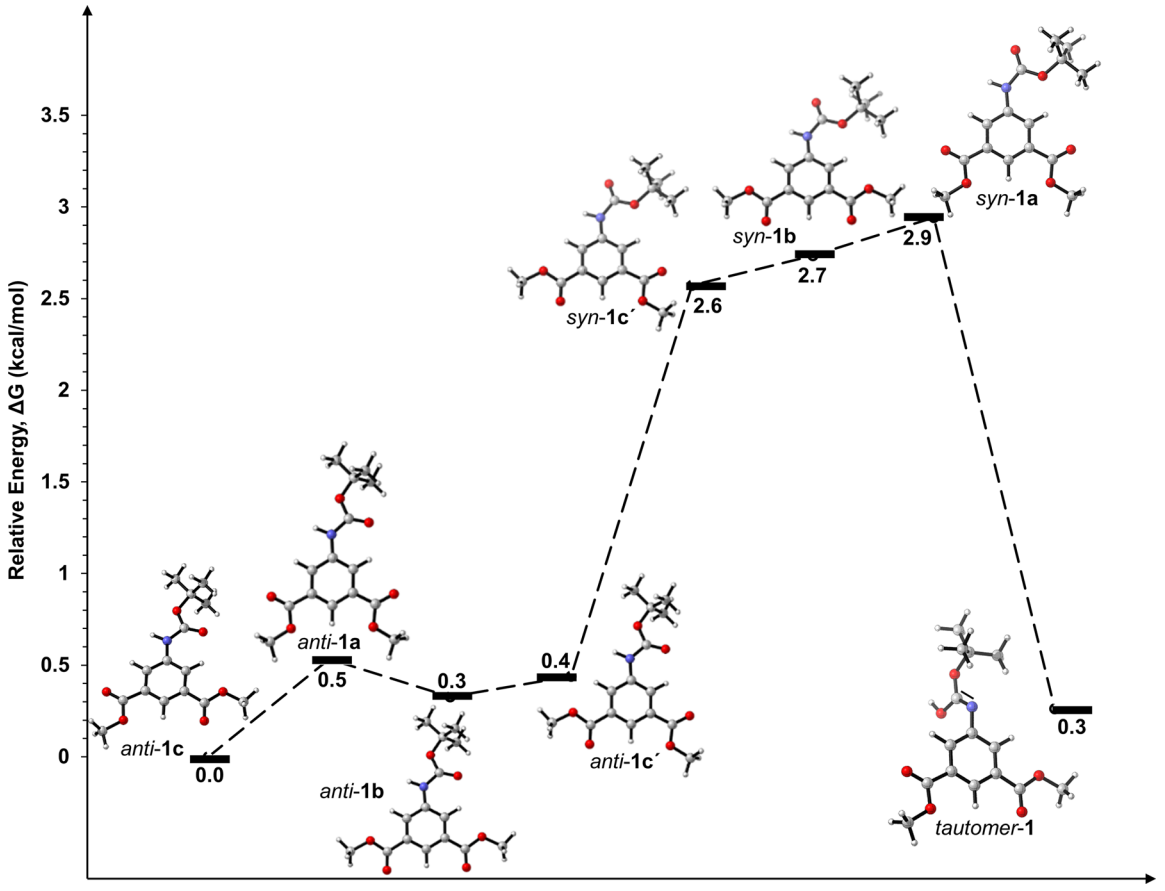

Figure 4. Computed energy diagram for the *anti*- and *syn*-rotamers and a tautomer of compound **1** calculated with Gaussian 16 with the B3LYP exchange-correlation functional and the polarized diffuse split-valence 6-311+G(d,p) basis set.

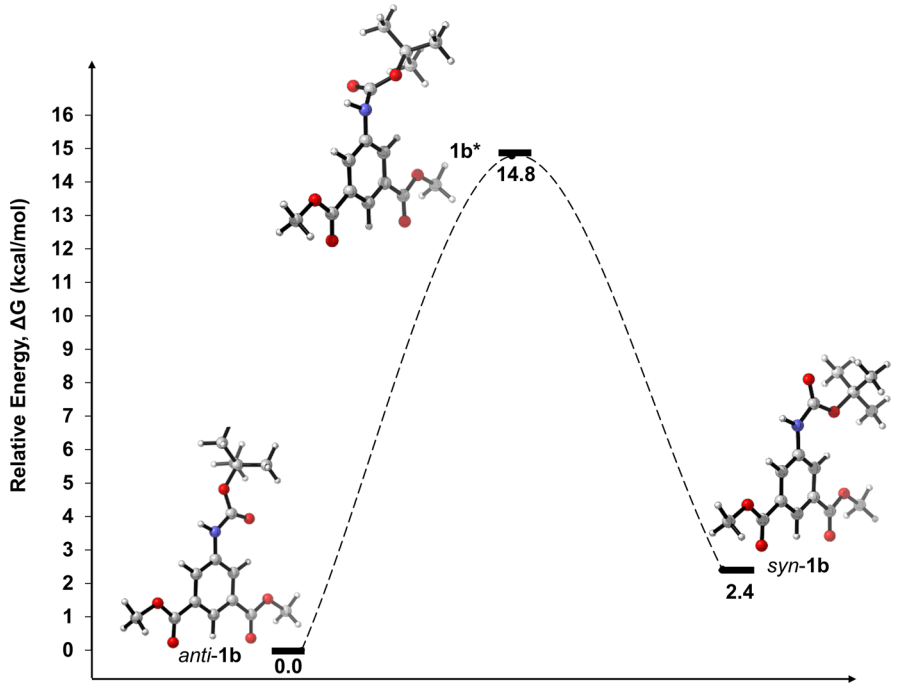

Figure 5. Computed energy diagram for the conversion of the *anti*-**1b** rotamer to the *syn*-**1b** rotamer via the transition state **1b***. The graphical depictions were generated using CYLview software.[1]

reacted with hydrazine hydrate and produced 5-amino isophthalic dihydrazide **2** in quantitative yield.

Computational Studies. Our computational investigation of the isomers of compound **1** supports the assignments made

https://dx.doi.org/10.1021/acs.bioconjchem.0c00590
Bioconjugate Chem. 2020, 31, 2789−2806

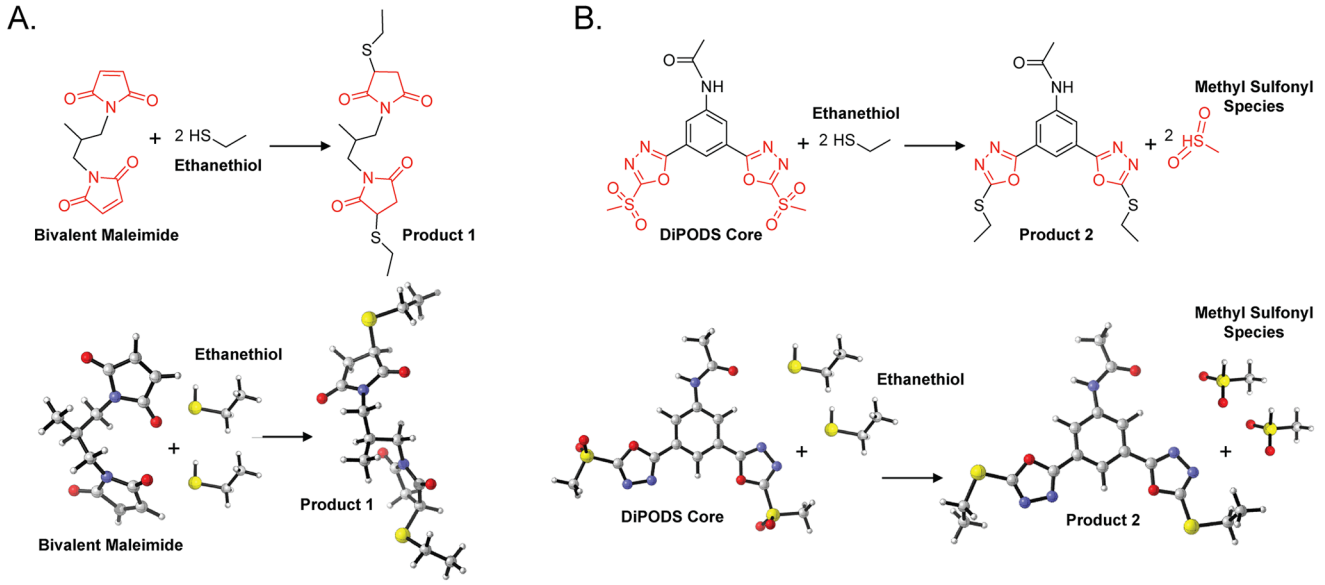

	Bivalent Maleimide	Ethanethiol	Product 1
G298 (kcal/mol)	-549091.3474	-299968.0886	-1149037.881
Total (kcal/mol)	-1149027.525		-1149037.881
E_P-E_{SM} (kcal/mol)	-10.35622844		

	DiPODS Core	Ethanethiol	Product 2	Methyl Sulfonyl
G298 (kcal/mol)	-1341679.713	-299968.0886	-1202227.052	-369700.6416
Total E (kcal/mol)	-1941615.89		-1941628.335	
E_P-E_{SM} (kcal/mol)	-12.44513625			

Figure 6. Computational investigation comparing the reactions between a pair of molecules of ethanethiol and (A) a bivalent maleimide-based probe and (B) DiPODS.

based on the VT-NMR data. The calculated Gibbs free energies of the rotamers of compound **1** revealed that the *anti*-rotamers are favored by ∼2.0 kcal/mol (Figure 4). Figure 4 shows the calculated structures of two groups of rotamers and a tautomer of compound **1**. The first group of rotamers includes four configurations of *anti*-rotamers (*anti*-**1a**, *anti*-**1b**, *anti*-**1c**, and *anti*-**1c′**) with energies similar to each other and to tautomer-**1**. The second group—which consists of three configurations of *syn*-rotamers (*syn*-**1a**, *syn*-**1b**, and *syn*-**1c′**) with similar energies—lies ∼2.0 kcal/mol higher than the *anti*-rotamers and the tautomer. The energy difference between the four *anti*-rotamers is very small (∼0.5 kcal/mol), suggesting they can interconvert at room temperature. This explains why they all manifest as a single set of signals (set **A**) in the ^{1}H NMR spectrum of compound **1** despite having different point group symmetries. Despite the calculated similarity in energy between the set **A** *anti*-rotamers and the imidic acid tautomer-**1** (Set **C**), they do not appear to interconvert at ambient temperature (Figure 2B). This suggests that a higher energy transition state must be passed for conversion, which is supported by the disappearance of the tautomer (set **C**) at elevated temperatures.

The interconversion between the *anti*- (set **A**) and *syn*- (set **D**) rotamers occurs via the rotation of the Boc group attached to the amine. In order to further understand this process, we calculated the transition state for one such rotation between *anti*-**1b** and *syn*-**1b** (Figure 5). To identify the transition state (**1b***), we started with the *anti*-**1b** rotamer, and the dihedral angle of interest was varied in a stepwise fashion toward that of the *syn*-**1b** rotamer using Spartan 14 software. The structure with the highest energy was carried forward for optimization as the transition state in Gaussian 16.[37] The harmonic vibrational frequencies showed only one imaginary frequency, corresponding to the desired transition. The energy difference between the transition state and the *anti*-**1b** rotamer is substantial (∼15 kcal/mol) and thus might not be overcome at room temperature, depending on other conditions such as solvent (Figure 5). One way to overcome this large energy barrier, however, is via heating, which could explain the formation of a separate set of ^{1}H NMR signals (set **D**) at elevated temperatures. It is important to note that the energy difference between the *syn*-rotamers is also small (∼0.3 kcal/mol), suggesting that they can interconvert easily at elevated temperatures and thus explaining their appearance as a single set of peaks in the ^{1}H NMR spectra.

Taken together, the aforementioned NMR and computational studies helped deconvolute the mixture of components formed when synthesizing compound **1**. Furthermore, these data help explain how this mixture of *anti*-rotamers, tautomer-**1**, and a doubly Boc-protected variant of compound **1** can react together to form compound **2** in near-quantitative yield: the elevated temperature of the reaction—90 °C for 3 days—would overcome any rotational energy barriers and allow for the production of compound **2** in quantitative yield.

Although these detailed VT-NMR and computational studies might appear to be more detail than needed for characterizing what could be viewed as a mere synthetic intermediate, we thought it prudent to better understand the behaviors of this molecule in terms of its observed conformers and the energetic barriers to its observed isomerization. The desired applications we are pursuing with DiPODS require it to react in a predictable and reproducible manner with two thiols. For example, if the reactivity were to be different for two rotamers/isomers of DiPODS, this could become an important physical property to understand. From our investigations, we believe the rotamer behavior appears to be largely the result of

https://dx.doi.org/10.1021/acs.bioconjchem.0c00590
Bioconjugate Chem. 2020, 31, 2789−2806

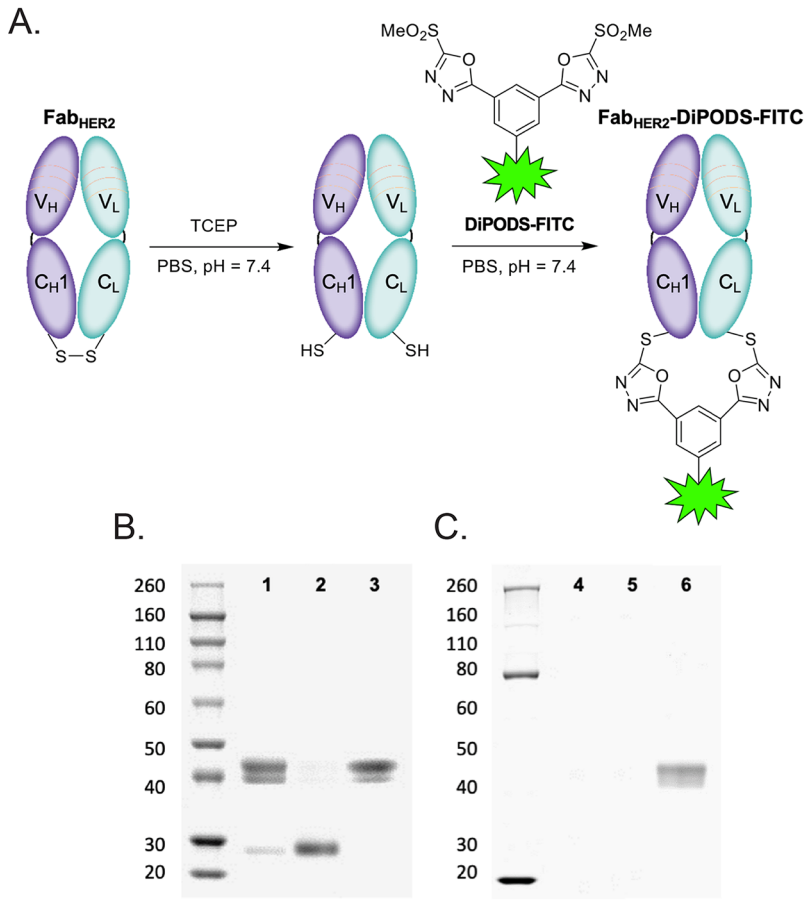

Figure 7. (A) Scheme of the site-specific conjugation of DiPODS-FITC to Fab$_{HER2}$. (B) SimplyBlue-staining of SDS-PAGE of the bioconjugation of DiPODS-FITC to Fab$_{HER2}$: (1) parent Fab$_{HER2}$; (2) reduced Fab$_{HER2}$; (3) Fab$_{HER2}$-DiPODS-FITC. (C) Fluorescence imaging of SDS-PAGE of the bioconjugation of DiPODS-FITC to Fab$_{HER2}$: (4) parent Fab$_{HER2}$; (5) reduced Fab$_{HER2}$; (6) Fab$_{HER2}$-DiPODS-FITC.

the Boc-protected amine and therefore not likely to be an issue for the final DiPODS compounds. Further, the imidic acid tautomer that we propose as set **C** is not likely to form in DiPODS itself or its derivatives, as the pK_a of the amide in these final conjugates is higher than that of the Boc-protected carbamate (which forms set **C**).

We also turned to computational methods to compare the thermodynamic stability of the conjugation product formed by DiPODS to those formed by a bivalent maleimide, a monovalent maleimide, and a monovalent PODS. To this end, ethanethiol was employed as a simple surrogate substrate, and the total energy of the final product(s) was compared to the total energy of the starting materials using the UAHF model for improved solvent modeling (Figures 6 and S1). Since all of the reactions were modeled as isodesmic, we were able to calculate the difference in total energy—i.e., Gibbs free energy—between the reactants and products in each case, thereby enabling a comparison between the net change in thermodynamic stability of each transformation. The ligation between ethanethiol and the monovalent maleimide resulted in a net Gibbs free energy change of −5.3 kcal/mol, while that between the same substrate and the monovalent PODS is slightly more stabilizing, with a net change of −5.6 kcal/mol (Figure S2). Not surprisingly, the divalent reagents created larger changes in free energy. More specifically, the reaction of the bivalent maleimide resulted in a change in Gibbs free energy of −10.3 kcal/mol, while the ligation between DiPODS and a pair of ethanethiol substrates provided an even greater gain in stability: −12.4 kcal/mol. While an extra ∼2.1 kcal/mol of stabilization does not represent a dramatic improvement, it—combined with the irreversibility of the DiPODS-based conjugation—certainly suggests that DiPODS-based conjugates will be more stable than their bismaleimide-based analogues both *in vitro* and *in vivo*.

Synthesis of a Fluorophore-Bearing Variant. DiPODS was designed to be modular, as its reactive primary amine facilitates the coupling of cargoes such as chelators, dyes, and toxins. In order to facilitate proof-of-concept reactivity and bioconjugation experiments, a fluorescein-bearing variant of DiPODS—DiPODS-FITC—was prepared via the reaction of DiPODS-PEG$_4$-NH$_2$ with fluorescein isothiocyanate in the presence of DIEA (Scheme 3).

Reactivity with a Model Thiol. *N*-Acetyl-L-cysteine methyl ester was used as a model thiol to evaluate the reactivity of DiPODS-FITC (Scheme S1). To this end, DIPODS-FITC was incubated at room temperature with 10 equiv of *N*-acetyl-L-cysteine methyl ester and 5 equiv of a mild reducing agent, tris(2-carboxyethyl)-phosphine (TCEP). The progress of the reaction was interrogated via LC-MS 5 min after mixing, and quantitative conversion to DiPODS-FITC-Cys$_2$ was observed (Figures S4 and S5).

Bioconjugation and Characterization. Fab fragments—rather than full-length IgGs—were selected for our proof-of-concept bioconjugation experiments with DiPODS-FITC

https://dx.doi.org/10.1021/acs.bioconjchem.0c00590
Bioconjugate Chem. 2020, 31, 2789−2806

because of the presence of only a single interchain disulfide linkage (rather than 8) dramatically simplifies the analysis of the products. In practice, two Fabs were employed: a commercially available, nonspecific Fab based on human plasma IgG (Fab_{ns}) and a HER2-targeting Fab created via the enzymatic digestion of trastuzumab (Fab_{HER2}). In each case, the Fab was first treated with TCEP to reduce the interchain disulfide bridge and then incubated with DiPODS-FITC (Figure 7A). Ultimately, the following optimal reaction conditions were identified: 2 h at 37 °C with 20 equiv of TCEP followed by 16 h with 15 equiv of DiPODS-FITC at the same temperature. Subsequently, UV−vis spectrophotometry was used to measure the degree of labeling (DOL) of each immunoconjugate, revealing that Fab_{ns}-DiPODS-FITC and Fab_{HER2}-DiPODS-FITC were modified with 0.86 ± 0.02 and 0.95 ± 0.01 FITC/Fab, respectively (Table 1). MALDI-TOF mass spectrometry confirmed a degree of labeling of ∼1 for each fluorophore-modified Fab (Figure S3).

Table 1. Bioconjugation Results Obtained Using DiPODS-FITC in Conjunction with Fab_{HER2} and Fab_{ns}

sample	HS-/Fab ratio	FITC/Fab ratio
parent Fab_{ns}	undetected	-
reduced Fab_{ns}	2.01 ± 0.12	-
Fab_{ns}-DIPODS-FITC	undetected	0.86 ± 0.02
parent Fab_{HER2}	undetected	-
reduced Fab_{HER2}	1.94 ± 0.10	-
Fab_{HER2}-DIPODS-FITC	undetected	0.95 ± 0.01

The stepwise progress of the bioconjugation procedure was monitored using both gel electrophoresis and Ellman's reagent, a chemical tool for the detection of free thiols. In the case of Fab_{HER2}, for example, the former illustrates the decoupling of the intact fragment's V_HC_{H1} and V_LC_L chains upon reduction with TCEP (Figure 7B, lanes 1 and 2) and the subsequent reunification of the two domains after treatment with DiPODS-FITC (Figure 7B, lane 3). The analysis of the gel using a fluorescence imager reveals only a single fluorescent band corresponding to an intact, 40−50 kDa Fab and does not show any multimeric cross-bridged species (i.e., Fab-DiPODS-Fab) (Figure 7C). The use of Ellman's reagent to assess the number of free thiols present at different points of the procedure reinforced the quantitative nature of the approach. The purified Fab_{HER2} starting material contains no detectable free thiols. Reduction with TCEP creates the expected maximum of 1.94 ± 0.11 thiols/Fab, a value which went back to effectively zero upon cross-bridging with DiPODS-FITC (Table 1). Importantly, both analytical techniques provided similar results for the bioconjugation of Fab_{ns}.

Next, circular dichroism (CD) spectroscopy was employed to interrogate the structure and melting point of Fab_{HER2}, reduced Fab_{HER2}, and Fab_{HER2}-DiPODS-FITC. Generally speaking, the spectra—which exhibit a positive peak around 205 nm and shallow negative peak around 217 nm—are characteristic of a protein rich in β-sheet content, consistent with the known secondary structure of Fab fragments (Figure S40). The data suggest that the trio of constructs have similar overall structures: the far-UV CD spectra of all three samples have the same shape profile, with only minor differences in ellipticity values which may reflect local conformational adjustments due to the reduction or rebridging of the disulfide bonds. Importantly, the CD data also indicate that the three fragments also share similar thermal stability, as the melting temperatures for Fab_{HER2}, reduced Fab_{HER2}, and Fab_{HER2}-DiPODS-FITC are 65.5, 66.8, and 64.5 °C, respectively, when monitored at 205 nm (Figure S41).

Finally, in order to assess the serum stability of Fab_{ns}-DiPODS-FITC and Fab_{HER2}-DiPODS-FITC, the fragments were incubated in 50% human serum albumin (HSA) for 7 days at 37 °C. Size exclusion HPLC of each fluorophore-bearing fragment after 7 days yielded a single, unchanged peak (Figure S6). Neither aggregates nor separate V_HC_{H1}/V_LC_L chains nor free fluorophores could be observed, underscoring the stability of the FITC-modified immunoconjugates and the irreversibility of the DiPODS linkage.

***In Vitro* Evaluation.** With the chemical characterization of Fab_{HER2}-DiPODS-FITC complete, the next step was to ensure that the immunoconjugate retained its ability to bind its molecular target. To this end, we performed flow cytometry

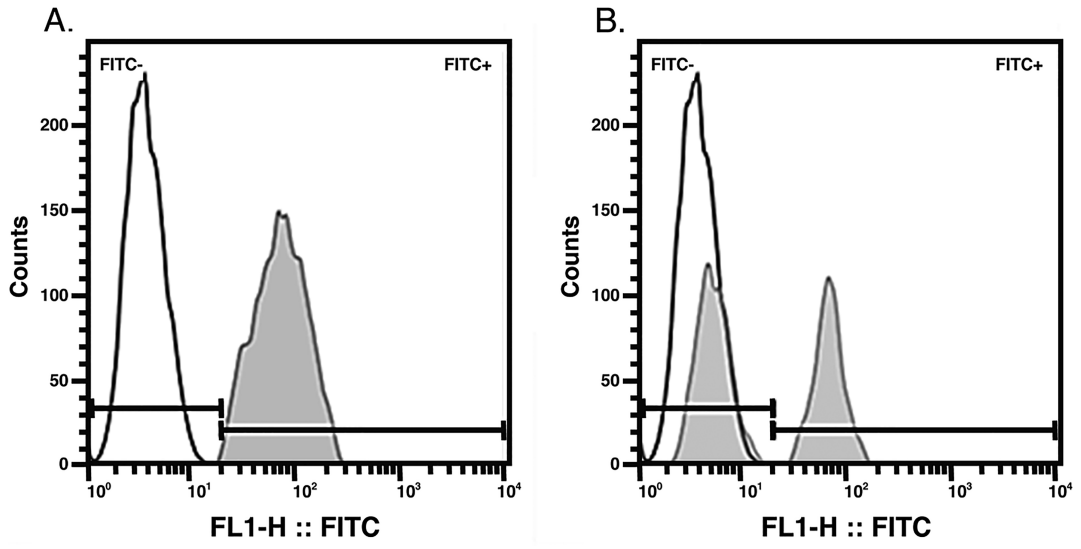

Figure 8. Flow cytometry analysis of HER2-positive BT474 human breast cancer cells stained with (A) Fab_{HER2}-DiPODS-FITC and (B) Fab_{HER2}-Lys-FITC.

https://dx.doi.org/10.1021/acs.bioconjchem.0c00590
Bioconjugate Chem. 2020, 31, 2789−2806

experiments using two human breast cancer cell lines: HER2-positive BT474 cells and HER2-negative MDA-MB-235 cells. As a point of comparison, a non-site-specifically modified, HER2-targeting immunoconjugate (Fab_{HER2}-Lys-FITC) was synthesized using a traditional lysine-based approach to bioconjugation and used alongside Fab_{HER2}-DiPODS-FITC in all cell cytometry experiments. The *in vitro* experiments clearly confirm the specificity of both immunoconjugates, as binding was observed with HER2-positive BT474 cells but not HER2-negative MDA-MB-231 cells. Just as important, however, are the differences between the behavior of the two FITC-modified Fabs and HER2-positive BT474 cells. Under identical conditions—i.e., concentration of cells, concentration of fragments, incubation time—only a single population of fluorophore-positive cells were detected after incubation with Fab_{HER2}-DiPODS-FITC, but both fluorophore-positive *and* fluorophore-negative cells were observed after incubation with Fab_{HER2}-Lys-FITC (Figure 8).

These data indicate that the immunoroeactivity of Fab_{HER2}-DiPODS-FITC is higher than that of Fab_{HER2}-Lys-FITC, most likely because the heterogeneous mixture of products that comprises the latter includes immunoconjugates in which fluorophores have been inadvertently appended to the antigen-binding domain of the fragment. These data serve as a reminder that the benefits of site-specific bioconjugation extend beyond simply producing better-defined and more homogeneous immunoconjugates.

CONCLUSION

In the preceding pages, we have described the synthesis, chemical characterization, computational investigation, and biological evaluation of DiPODS, a reagent for site-specific bioconjugation bearing two thiol-reactive oxadiazolyl methyl sulfones. Where maleimide−thiol conjugations form reversible and labile linkages, DiPODS−thiol conjugations form strong and irreversible linkages. Proof-of-concept bioconjugation experiments with a pair of Fab fragments demonstrate that DiPODS reliably facilitates the construction of stable and homogeneous immunoconjugates via the rebridging of interchain disulfide bonds. Moreover, flow cytometry experiments with human breast cancer cells illustrate that a fluorescent, HER2-targeting immunoconjugate synthesized using DiPODS exhibits superior *in vitro* performance compared to an analogous construct synthesized via a non-site-specific, lysine-based approach to bioconjugation. Efforts to leverage DiPODS for the construction of immunoconjugates based on full-length IgGs are already underway, and in the near future we plan to exploit the modularity of DiPODS to create derivatives bearing bifunctional chelators for the construction of immunoconjugates for PET, SPECT, and targeted endoradiotherapy.

MATERIALS AND METHODS

Reagents. Unless otherwise stated, all chemicals and reagents were obtained commercially and used without further purification. 1-Ethyl-3-(3-(dimethylamino)propyl)-carbodiimide hydrochloride (EDC), carbon disulfide, peptide synthesis-grade *N*,*N*-diisopropylethylamine (DIEA), triethylamine, sodium hydroxide (NaOH), and trifluoroacetic acid (TFA) were purchased from Fisher Scientific. 4-(Dimethylamino)pyridine, hydrazine hydrate, iodomethane, and oxyma pure were purchased from Sigma-Aldrich. Dimethyl 5-aminoisophthalate was purchased from Alpha-Aesar. Di-*tert*-butyl decarbonate and 3-chloroperoxybenzoic acid (*m*CPBA) were purchased from AK Scientific. Fluorescein isothiocyanate isomer I and *t*-Boc-*N*-amido-PEG_4-acid were purchased from BroadPharm. All chemicals for the *in vitro* and *in vivo* experiments, unless otherwise noted, were acquired from Sigma-Aldrich and used as received without further purification. All water used was ultrapure (>18.2 MΩ cm^{-1}), and dimethyl sulfoxide was of molecular biology grade (>99.9%). The unconjugated Fab_{HER2} and was provided by Rockland Immunochemicals, Inc. (Pottstown, PA).

Characterization Methods. ^1H and ^{13}C NMR spectra were recorded on a 500 MHz Bruker Avance NMR spectrometer at 25 °C in [D_6]DMSO. Variable temperature ^1H NMR were recorded on a Bruker Avance III HD 600 MHz spectrometer. ^1H chemical shifts were referenced to the residual protons of the deuterated [D_6]DMSO solvent at δ = 2.50 ppm;[38] ^{13}C chemical shifts were referenced to the [D_6]DMSO signal at δ = 39.52 ppm.[39] Coupling constants are reported to the nearest 0.5 Hz (^1H NMR spectroscopy) or rounded to integer values in Hz (^{13}C NMR spectroscopy). Assignments were supported by additional NMR experiments (DEPT135, HMQC, COSY). High-resolution mass spectra were measured on a JEOL AccuTOF GCv 4G using field desorption ionization (FDI). For the isotopic pattern only, the mass peak of the isotopologue or isotope with the highest natural abundance is given. Low resolution mass spectrometry and LCMS was performed using an Advion Expression-L system (mass range <2000 amu). FTIR spectroscopy was performed using a Bruker Tensor 27 FT-IR spectrometer equipped with ATR attachment and OPUS data collection program. HPLC purifications were performed using a ThermoFisher Vanquish HPLC equipped with C18 reversed-phase column (Spursil Semipreparative DIKMA; 5 μm, 21.2 × 250 mm), a VF-D40-A UV detector, two VF-P10-A pumps, a Chromeleon 7 communication software, and a ThermoFisher DIONEX UltiMate 3000 fraction collector, using a flow rate of 8 mL/min and a gradient of MeCN:H_2O (both with 0.1% TFA). Compounds **5**, **6**, **8**, **9**, and **10** were only characterized using ^1H NMR spectroscopy and low-resolution mass spectrometry, as they were only used toward developing an optimized procedure.

Chemical Syntheses. *Synthesis of 5-[[(1,1-Dimethylethoxy)carbonyl]amino]-1,3-dimethyl ester (**1**).* Compound **1** was prepared according to a published procedure with some alteration.[34] Using Schlenk techniques, portions of commercially procured dimethyl 5-aminoisophthalate (3.00 g, 14.34 mmol) and 4-(dimethylamino)pyridine (2.24 g, 18.36 mmol) were purged with N_2 gas, transferred to a reaction vessel under N_2 gas, and dissolved in anhydrous THF (50.0 mL). The clear yellow mixture was cooled to 0 °C prior to the addition of di-*tert*-butyl dicarbonate (4.00 mL, 17.50 mmol); upon which a thick, white precipitate formed inside the reaction vessel. The reaction mixture was kept under N_2 flow as it initially stirred at 0 °C (ice bath) and gradually warmed to room temperature as the ice bath melted and the reaction proceeded over 24 h. Volatiles were removed by rotary evaporation under vacuum before reconstituting the mixture with EtOAc (100 mL). The organic solution was washed twice with 0.5 N HCl (2 × 100 mL), three times with brine solution (3 × 100 mL), and deionized water (100 mL) to achieve a neutral pH. The organic layer was dried over Na_2SO_4 before removing the solvent under reduced pressure to yield a mixture

https://dx.doi.org/10.1021/acs.bioconjchem.0c00590
Bioconjugate Chem. 2020, 31, 2789−2806

of the product as an off-white solid with negligible amounts of the Boc-deprotected starting material observed by ^{1}H NMR (4.72 g, 106%). The crude mixture was purified by column chromatography to isolate the major component from the mixture (3.28 g, 74%). However, it was later determined that the crude product could be used without further purification for the added benefit of increased yields for the production of compound **2**. ^{1}H NMR of the crude mixture (500 MHz, [D_6]DMSO, 25 °C, TMS): set **A** (*anti*-rotamers, *anti*-**1**) δ = 1.49 [s, 9H; $NHCO_2C(C\underline{H}_3)_3$], 3.88 (s, 6H; $CO_2C\underline{H}_3$), 8.08 (t, J = 1.4 Hz, 1H; Ar-C<u>H</u>), 8.36 (m, 2H; Ar-C<u>H</u>), 9.89 (br, 1H; N<u>H</u>) ppm; set **B** [doubly Boc-protected derivative of compound **1**, $(Boc)_2$-**1**]: δ = 1.39 {s, 18H; $N[CO_2C(C\underline{H}_3)_3]_2$}, 3.90 [s, 6H; $CO_2C\underline{H}_3$], 8.01 (d, J = 1.5 Hz, 2H; Ar-C<u>H</u>), 8.41 (t, J = 1.5 Hz, 1H; Ar-C<u>H</u>) ppm; set **C** (tautomers of compound **1**, tautomer-**1**): δ = 1.42 [s, 9H; $NC(OH)OC(C\underline{H}_3)_3$], 3.91 (s, 6H; $CO_2C\underline{H}_3$), 8.17 (d, J = 1.5 Hz, 1H; Ar-C<u>H</u>), 8.45 (t, J = 1.5 Hz, 2H; Ar-C<u>H</u>) ppm; ^{13}C{^{1}H} NMR of the crude mixture (126 MHz, [D_6]DMSO, 25 °C, TMS): set **A** (*anti* rotamers, *anti*-**1**): δ = 28.1 [$NHCO_2C(\underline{C}H_3)_3$], 52.5 ($CO_2\underline{C}H_3$), 79.9 [$NHCO_2\underline{C}(CH_3)_3$], 122.5, 123.0 (Ar-<u>C</u>H), 130.6 (Ar-<u>C</u> attached to CO_2CH_3), 140.7 [Ar-<u>C</u> attached to $NHCO_2C(CH_3)_3$], 152.7 [$NH\underline{C}O_2C(CH_3)_3$], 165.4 ($\underline{C}O_2CH_3$) ppm; Signals associated with set **B** [doubly Boc-protected derivative of compound **1**, $(Boc)_2$-**1**], and set **C** (imidic acid tautomers of compound **1**, tautomer-**1**) of the crude mixture could not be distinguished from one another by ^{13}C NMR techniques and are reported together herein. Crude mixture sets **B** and **C**: δ = 27.5, 27.5 {$N[CO_2C(\underline{C}H_3)_3]_2$} and $NC(OH)OC(\underline{C}H_3)_3$], 52.8, 52.8 ($CO_2\underline{C}H_3$), 83.1, 84.4 {$N[CO_2\underline{C}(CH_3)_3]_2$} and [$NC(OH)O\underline{C}(CH_3)_3$], 128.3, 128.8 (Ar-<u>C</u>H), 131.0, 131.2 (Ar-<u>C</u> attached to CO_2CH_3), 133.0, 133.1 (Ar-<u>C</u>H), 139.5, 140.0 [Ar-<u>C</u> attached to {$N[CO_2C(CH_3)_3]_2$} and $NC(OH)OC(CH_3)_3$], 150.6, 150.8 {$N[\underline{C}O_2C(CH_3)_3]_2$} and [$N\underline{C}(OH)OC(CH_3)_3$], 164.7, 164.8 [$(\underline{C}O_2CH_3)_2$] ppm; HRMS (FDI): m/z calcd. for $C_{15}H_{19}NO_6$: 309.11977[M]$^+$; found: 309.11989; m/z calcd. for $C_{20}H_{27}NO_8$+Boc: 409.17815[M+Boc]$^+$; found: 409.17820; IR (FTIR): $\tilde{\nu}$ = 3364.40 (w) [$NHCO_2C(CH_3)_3$, N−H], 2980.61 (w), 2954.57 (w) [{$N[CO_2C(CH_3)_3]_2$} and $NC(OH)OC(CH_3)_3$, C−H], 2360.57 (w), 2339.30 (w) [$NC(OH)OC(CH_3)_3$, N═C], 1741.50 (m), 1726.07 (s), 1704.85 (s) [CO_2CH_3, C═O] 1604.57 (w), 1549.61 (m) cm^{-1} [{$N[CO_2C(CH_3)_3]_2$}, C═O].

The major component of the compound **1** product mixture, *anti*-rotamers (*anti*-**1**, set **A**), was isolated from the crude mixture for further analysis via precipitation. The crude product (2.51 g, 8.12 mmol) was dissolved completely in a minimal amount of warm DCM and stored at −20 °C overnight. The *anti*-rotamers of compound **1** (*anti*-**1**, set **A**) were precipitated under the aforementioned storage conditions and were isolated from the mother liquor as a shiny white precipitate after vacuum filtration. The mother liquor was collected after vacuum filtration and subjected to rotary evaporation to remove solvent residues. The residual solids were redissolved in minimal amounts of warm DCM to repeat the precipitation process. Precipitation of the *anti*-rotamers of compound **1** (*anti*-**1**, set **A**) was repeated several times until a pure product could no longer be isolated from the mother liquor solution (*anti*-**1**, set **A**: 1.56 g, 66%). ^{1}H NMR of *anti*-**1**, set **A** (500 MHz, [D_6]DMSO, 25 °C, TMS): δ = 1.49 [s, 9H; $NHCO_2C(C\underline{H}_3)_3$], 3.88 (s, 6H; $CO_2C\underline{H}_3$), 8.08 (t, J = 1.4 Hz, 1H; Ar-C<u>H</u>), 0.8.35 (d, J = 0.86 Hz, 2H; Ar-C<u>H</u>), 9.87 (br, 1H; N<u>H</u>) ppm; ^{13}C{^{1}H} NMR of *anti*-**1**, set **A** (126 MHz, [D_6]DMSO, 25 °C, TMS): δ = 28.0 [$NHCO_2C(\underline{C}H_3)_3$], 52.5 ($CO_2\underline{C}H_3$), 79.9 [$NHCO_2\underline{C}(CH_3)_3$], 122.4, 123.0 (Ar-<u>C</u>H), 130.6 (Ar-<u>C</u> attached to CO_2CH_3), 140.6 [Ar-<u>C</u> attached to $NHCO_2C(CH_3)_3$], 152.7 [$NH\underline{C}O_2C(CH_3)_3$], 165.4 ($\underline{C}O_2CH_3$) ppm; HRMS (FDI): m/z calcd. for $C_{15}H_{19}NO_6$: 309.11977[M]$^+$; found: 309.12124; IR (FTIR): $\tilde{\nu}$ = 3363.43 (m) [$NHCO_2C(CH_3)_3$, N−H], 2952.65 (b) [$NHCO_2C(CH_3)_3$, C−H], 1718.36 (m), 1703.89 (s) (CO_2CH_3, C═O), 1608.43 (m), 1545.75 (s) cm^{-1}(Ar-CH).

Synthesis of Compound 2. Hydrazine hydrate (28.0 mL, 451 mmol) was added to a clear colorless solution of compound **1** (3.49 g, 11.28 mmol) in EtOH (150 mL) at room temperature. The color of the solution turned a pale-yellow. The mixture was refluxed at 90 °C for 3 days. All volatiles were removed under reduced pressure to yield quantitative amounts of the product, compound **2**, in the form of a fine, matte-white powder (3.49 g, quantitative yield). The product material was used without further purification to proceed forward with the synthesis of compound **3**. ^{1}H NMR (500 MHz, [D_6]DMSO, 25 °C, TMS): δ = 1.48 [s, 9H; $NHCO_2C(C\underline{H}_3)_3$], 4.49 (br, 4H; $CONHN\underline{H}_2$), 7.74 (t, J = 1.4 Hz, 1H; Ar-C<u>H</u>), 7.96 (d, J = 1.0 Hz, 2H; Ar-C<u>H</u>), 9.64 (br, 3H; N<u>H</u>) ppm; ^{13}C{^{1}H} NMR (126 MHz, [D_6]DMSO, 25 °C, TMS): δ = 28.1 [$NHCO_2C(\underline{C}H_3)_3$], 79.5 [$NHCO_2\underline{C}(CH_3)_3$], 118.8, 119.6 (Ar-<u>C</u>H), 134.3 (Ar-<u>C</u> attached to $CONHNH_2$), 139.8 [Ar-<u>C</u> attached to $NHCO_2C(CH_3)_3$], 152.8 [$NH\underline{C}O_2C(CH_3)_3$], 165.8 ($\underline{C}ONHNH_2$) ppm; HRMS (FDI): m/z calcd. for $C_{13}H_{19}N_5O_4$: 309.14491[M]$^+$; found: 309.14370.

Synthesis of Compound 3. Potassium hydroxide (1.686 g, 29.16 mmol) was added to a suspension of compound **2** (4.14 g, 13.25 mmol) in EtOH (130 mL) and stirred for 10 min. Carbon disulfide (17.5 mL, 291.5 mmol) was added dropwise to this emulsion. The reaction mixture turned yellow followed by formation of a large amount of precipitate. The reaction mixture was heated to reflux at 90 °C for 16 h. Upon refluxing, the reaction mixture became a clear pale-yellow solution with small amount of white precipitate. After cooling the reaction mixture to room temperature, EtOAc (320 mL) was added until complete dissolution of the precipitate material was achieved. The resulting clear yellow mixture was washed two times with 1 M HCl (2 × 320 mL) followed by washing 3 times with deionized water (3 × 320 mL) to achieve a neutral pH. The yellow organic layer was washed with brine (320 mL), and then dried over Na_2SO_4. All volatiles were removed under reduced pressure; yielding compound **3** as shiny white solid (4.73 g, 91% yield). ^{1}H NMR (500 MHz, [D_6]DMSO, 25 °C, TMS): δ = 1.51 [s, 9H; $NHCO_2C(C\underline{H}_3)_3$], 7.82 (t, J = 1.5 Hz, 1H; Ar-C<u>H</u>), 8.22 (d, J = 1.0 Hz, 2H; Ar-C<u>H</u>), 10.05 (br, 1H; N<u>H</u>), 14.75 (br, 2H; S<u>H</u>) ppm; ^{13}C{^{1}H} NMR (126 MHz, [D_6]DMSO, 25 °C, TMS): δ = 28.0 [$NHCO_2C(\underline{C}H_3)_3$], 80.3 [$NHCO_2\underline{C}(CH_3)_3$], 116.2, 117.5 (Ar-<u>C</u>H), 124.2 (Ar-<u>C</u> attached to C_2N_2O), 141.5 [Ar-<u>C</u> attached to $NHCO_2C(CH_3)_3$], 152.7 [$NH\underline{C}O_2C(CH_3)_3$], 159.4 ($\underline{C}_2N_2O$ attached to Ar), 177.5 ($\underline{C}_2N_2O$ attached to SH) ppm; HRMS (FDI): m/z calcd. for $C_{15}H_{15}N_5O_4S_2$: 393.05703[M]$^+$; found: 393.05654.

Synthesis of Compound 4. Triethylamine (3.39 mL, 24.2 mmol) was added to a clear yellow solution of compound **3** (2.63 g, 6.68 mmol) in dry THF (63.5 mL). After 10 min of stirring at room temperature, the color of the reaction mixture changed to a peach hue. To prevent light-sensitive reagents from degrading, the reaction vessel was covered with

https://dx.doi.org/10.1021/acs.bioconjchem.0c00590
Bioconjugate Chem. 2020, 31, 2789−2806

aluminum foil. Iodomethane (1.11 mL, 17.8 mmol) was slowly added to the reaction mixture and reacted for 3 h at room temperature. During the first 1−2 min of stirring, the clear peach solution quickly became opaque with white precipitate. Once the reaction was completed, the THF solvent was removed *in vacuo* to afford a mixture of white and tan colored solids. A crude form of the product material was extracted from the mixture with EtOAc (500 mL). The solution volume was reduced to 1/3 by evaporating volatiles under reduced pressure. This mixture was washed with a 0.1 M aqueous solution of Na_2CO_3 (2 × 100 mL) (pH = 11). The deep-yellow organic phase was washed with brine (150 mL) and deionized water until a neutral pH was achieved. As the organic layer was neutralized, its coloring changed from deep-yellow to a clear pale yellow. The organic phase was dried over Na_2SO_4 and filtered before removing solvent under reduced pressure. Product **4** was obtained as an off-white powder (2.61 g, 93% yield). ^{1}H NMR (500 MHz, [D_6]DMSO, 25 °C, TMS): δ = 1.51 [s, 9H; $NHCO_2C(C\underline{H}_3)_3$], 2.79 (s, 6H; $SC\underline{H}_3$), 8.00 (t, J = 1.43 Hz, 1H; Ar-C$\underline{H}$), 8.30 (m, 2H; Ar-C$\underline{H}$), 9.99 (br, 1H; N$\underline{H}$) ppm; ^{13}C{^{1}H} NMR (126 MHz, [D_6]DMSO, 25 °C, TMS): δ = 14.4 ($S\underline{C}H_3$), 28.0 [$NHCO_2C(\underline{C}H_3)_3$], 80.2 [$NHCO_2\underline{C}(CH_3)_3$], 116.9, 117.7 (Ar-$\underline{C}$H), 124.7 (Ar-$\underline{C}$ attached to C_2N_2O), 141.5 [Ar-$\underline{C}$ attached to $NHCO_2C(CH_3)_3$], 152.7 [$NH\underline{C}O_2C(CH_3)_3$], 164.2 ($\underline{C}_2N_2O$ attached to Ar), 165.3 ($\underline{C}_2N_2O$ attached to SCH_3) ppm; HRMS (FDI): m/z calcd. for $C_{17}H_{19}N_5O_4S_2$: 421.08627[M]$^+$; found: 421.08784.

Synthesis of Compound ***5***. At 0 °C, *m*CPBA (365.0 mg, 1.6 mmol) was added slowly into a clear yellow solution of compound **4** (101.1 mg, 0.240 mmol) in dry DCM (6.0 mL). The reaction mixture stirred overnight at room temperature. It formed a suspension with a lot of precipitate. The mixture was quenched with an aqueous solution of $NaHCO_3$. The aqueous phase was washed several times with DCM. The combined organic phase was washed with brine, dried over Na_2SO_4, and filtered before removing all volatiles under reduced pressure. The crude product was dissolved in a solvent mixture (17.0 mL) of MeCN:H_2O (3:1) for HPLC purification. Compound **5** was isolated by semipreparative RP-HPLC purification as a white solid (88.3 mg, 77%). ^{1}H NMR (500 MHz, [D_6]DMSO, 25 °C, TMS): δ = 1.52 [s, 9H; $C(C\underline{H}_3)_3$], 3.74 (s, 6H; $SO_2C\underline{H}_3$), 8.26 (m, 1H; Ar-C$\underline{H}$), 8.53 (m, 2H; Ar-C$\underline{H}$), 10.16 (br, 1H; N$\underline{H}$Boc) ppm. As compound **5** was only used for developing the optimized procedure, it was not fully characterized. The identity of compound **5** was confirmed with LR-mass spectrometry and ^{1}H NMR spectroscopy.

Synthesis of Compound ***6***. Compound **5** (15.6 mg, 0.032 mmol) was dissolved in a 1:1 mixture of TFA:DCM (2 mL). It was stirred for 3 h at room temperature. The reaction solvent was removed under reduced pressure, while the majority of TFA was removed azeotropically by washing the reaction mixture several times with toluene. Compound **6** was obtained as a yellowish white solid (9.2 mg, 74%). ^{1}H NMR (500 MHz, [D_6]DMSO, 25 °C, TMS): δ = 3.72 (s, 6H; $SO_2C\underline{H}_3$), 6.19 (br, 2H; $N\underline{H}_2$), 7.57 (m, 2H; Ar-C$\underline{H}$), 7.80 (m, 1H; Ar-C$\underline{H}$) ppm. As compound **6** was only used for developing the optimized procedure, it was not fully characterized. The identity of compound **6** was confirmed with LR-mass spectrometry and ^{1}H NMR spectroscopy.

Synthesis of Compound ***7***. Compound **4** (0.310 g, 0.712 mmol) was dissolved in a 1:1 mixture of TFA:DCM (16.0 mL). The mixture was stirred for 3 h at room temperature. The reaction solvent was removed under reduced pressure, while the majority of TFA was removed azeotropically by washing the reaction mixture several times with toluene. The crude product was washed with a 5:2 mixture of MeCN:H_2O and centrifuged at 4700 rpm for 9 min; yielding an off-white pellet and clear yellow solution. The pellet was washed twice with deionized water (2 × 20 mL) and freeze−dried for 24 h to afford compound 7 as a fine, off-white powder (0.154 g, 67%). ^{1}H NMR (500 MHz, [D_6]DMSO, 25 °C, TMS): δ = 2.77 (s, 6H; $SC\underline{H}_3$), 5.96 (br, 2H; $N\underline{H}_2$), 7.36 (d, J = 1.4 Hz, 1H; Ar-C$\underline{H}$), 7.56 (d, J = 1.4 Hz, 2H; Ar-C$\underline{H}$) ppm; ^{13}C{^{1}H} NMR (126 MHz, [D_6]DMSO, 25 °C, TMS): δ = 14.3 ($S\underline{C}H_3$), 110.5, 113.5 (Ar-$\underline{C}$H), 124.7 (Ar-$\underline{C}$ attached to C_2N_2O), 150.3 (Ar-$\underline{C}$ attached to NH_2), 164.8 ($\underline{C}_2N_2O$ attached to Ar), 164.8 ($\underline{C}_2N_2O$ attached to SCH_3) ppm; HRMS (FDI): m/z calcd. for $C_{12}H_{11}N_5O_2S_2$: 321.03545[M]$^+$; found: 321.03542.

Synthesis of Compound ***8***. Compound 7 (49.2 mg, 0.153 mmol) and succinic anhydride (46.6 mg, 0.466 mmol) were dissolved in dry THF (5.0 mL). To this clear yellow solution was added triethylamine (44 μL, 0.315 mmol) at room temperature. The reaction mixture was submerged into an oil bath and heated to 45 °C with stirring for 72 h at 45 °C. All volatiles were removed under reduced pressure. Deionized water (20.0 mL) was added to this solid residue and let stir for 2 min. It formed a suspension with white precipitate and colorless mother liquor. The white precipitate was further washed with deionized water until the mother liquor's pH = 7. The final precipitate was pelleted from the water via centrifugation, the water decanted, and the wet solid was freeze−dried for 24 h to afford compound **8** as a white solid (48.7 mg, 76%). ^{1}H NMR (500 MHz, [D_6]DMSO, 25 °C, TMS): δ = 2.56 [m, 2H; $NHCO(C\underline{H}_2)_2COOH$], 2.63 [m, 2H; $NHCO(C\underline{H}_2)_2COOH$], 2.78 (s, 6H; $SC\underline{H}_3$), 8.09 (m, 1H; Ar-C$\underline{H}$), 8.45 (m, 2H; Ar-C$\underline{H}$), 10.60 [br, 1H; N$\underline{H}$CO-$(CH_2)_2COOH$], 12.21 [br, 1H; $NHCO(CH_2)_2COO\underline{H}$] ppm. As compound **8** was only used for developing the optimized procedure, it was not fully characterized. The identity of compound **8** was confirmed with LR-mass spectrometry and ^{1}H NMR spectroscopy.

Synthesis of Compound ***9***. A solution of HATU (45.7 mg, 0.120 mmol) and DIEA (0.05 mL, 0.287 mmol) in a 1:2 solvent mixture of DMF:DCM (3 mL) was added to a solution of compound **8** (43.3 mg, 0.103 mmol) in a 1:1 solvent mixture of DMF:DCM (2 mL). This solution was added to a solution of $BocNH(PEG)_3NH_2$ (32.6 mg, 0.111 mmol) in DCM (2.2 mL). The reaction mixture was stirred at room temperature for 18 h followed by stirring at 50 °C for 3 h. All volatiles were removed under reduced pressure to form a brownish residue. To this residue was added deionized water (1 mL) and MeCN (5 mL) followed by vigorous stirring for 2 min. A large quantity of precipitate was formed with a brown mother liquor remaining. The mother liquor was decanted, and the precipitate was washed several times with MeCN until the mother liquor remained colorless. The final precipitate was dried under high vacuum, which afford compound **9** (13.0 mg) as a white solid. All volatiles were removed from mother liquor mixture. It was redissolved in a solvent mixture (13.0 mL) of MeCN:H_2O (5:8) for a HPLC purification. More of compound **9** (10.1 mg) by semipreparative RP-HPLC purification was isolated as the major component of the mother liquor mixture by HPLC purification. ^{1}H NMR (500 MHz, [D_6]DMSO, 25 °C, TMS): δ = 2.80 (s, 6H; $SC\underline{H}_3$), 2.82 [s, 4H; $N(CO)_2(C\underline{H}_2)_2$], 8.14 (m, 2H; Ar-C$\underline{H}$), 8.44 (m, 1H;

https://dx.doi.org/10.1021/acs.bioconjchem.0c00590
Bioconjugate Chem. 2020, 31, 2789−2806

Ar-CH) ppm. As compound **9** was only used for developing the optimized procedure, it was not fully characterized. The identity of compound **9** was confirmed with LR-mass spectrometry and ^{1}H NMR spectroscopy.

*Synthesis of Compound **10**.* EEDQ (19.1 mg, 0.077 mmol) was added to a solution of compound **8** (27.7 mg, 0.066 mmol) in a 1:1 solvent mixture of DMF:DCM (3 mL). BocNH(PEG)$_3$NH$_2$ (16.1 mg, 0.055 mmol) was added to this mixture after stirring for 50 min at room temperature. The reaction mixture was stirred at room temperature for 96 h. All volatiles were removed under reduced pressure. The solid residue was dissolved in DCM (1.0 mL) with 10% MeOH (0.1 mL) for automated flash column chromatography [Biotage column with silica; 100%MeCN → DCM+10%MeOH → DCM:MeOH (1:1)]. After column chromatography, three compounds were separated. The first collected fraction gave compound **9** (2.3 mg, 9%), the second collected fraction afforded the desired product, compound **10** (6.8 mg, <18%; note: product contained quinoline, a side product, as an impurity), and the third collected fraction was starting material, compound **8** (9.0 mg, 33%). ^{1}H NMR of compound **10** (500 MHz, [D$_6$]DMSO, 25 °C, TMS): δ = 1.36 [s, 9H; C(CH$_3$)$_3$], 2.45 [m, 2H, NH(CO)(CH$_2$)$_2$CONH-(OC$_2$H$_4$)$_3$NHBoc], 2.60 [m, 2H, NH(CO)(CH$_2$)$_2$CONH-(OC$_2$H$_4$)$_3$NHBoc], 2.79 (s, 6H; SCH$_3$), 3.05 (m, 2H; CH$_2$ of PEG), 3.20 (m, 2H; CH$_2$ of PEG), 3.36 (m, 2H; CH$_2$ of PEG), 3.40 (m, 2H; CH$_2$ of PEG), 3.46−3.52 (m, 8H; CH$_2$ of PEG), 6.76 [br, 1H, NH(CO)(CH$_2$)$_2$CONH-(OC$_2$H$_4$)$_3$NHBoc], 8.09 (m, 1H; Ar-CH), 8.45 (m, 2H; Ar-CH), 8.91 [br, 1H, NH(CO)(CH$_2$)$_2$CONH-(OC$_2$H$_4$)$_3$NHBoc], 10.52 [br, 1H, NH(CO)(CH$_2$)$_2$CONH-(OC$_2$H$_4$)$_3$NHBoc] ppm. As compound **10** was used only for developing the optimized procedure, it was not fully characterized. The identity of compound **10** was confirmed with LR-mass spectrometry and ^{1}H NMR spectroscopy.

*Synthesis of Compound **11**.* In a 50 mL Schlenck flask, compound **7** (105.7 mg, 0.329 mmol), EDC (86.0 mg, 0.45 mmol), and oxyma (70.6 mg, 0.497 mmol) were placed under vacuum for 30 min. The vessel was subsequently purged with N$_2$ gas and the reagent mixture was dissolved with anhydrous DMF (10.0 mL) to form a clear light-yellow solution. BocNH(PEG)$_4$COOH (108.6 mg, 0.297 mmol) was added to the reaction mixture at room temperature followed by addition of triethylamine (0.125 mL), which led to a change in color as the solution changed from yellow to orange. The mixture was heated at 50 °C for 48 h under N$_2$ flow. All volatiles were removed under high vacuum following the reaction and the resulting orange residue was dissolved in a solvent mixture (30.0 mL) of MeCN:H$_2$O (1:1) for a semipreparative RP-HPLC purification. Compound **11** was isolated by HPLC purification as a sticky pale yellow solid (110.7 mg, 55%). ^{1}H NMR (500 MHz, [D$_6$]DMSO, 25 °C, TMS): δ = 1.35 [s, 9H; C(CH$_3$)$_3$], 2.62 (t, J = 5.9 Hz, 2H; CH$_2$ of PEG), 2.79 [s, 6H; S(CH$_3$)], 3.03 (q, J = 5.8 Hz, 2H; CH$_2$ of PEG), 3.31−3.35 (m, 1H; CH$_2$ of PEG), 3.42−3.55 (m, 13H; CH$_2$ of PEG), 3.73 (t, J = 5.9 Hz, 2H; CH$_2$ of PEG), 6.73 (m, 1H; NHBoc), 8.09 (t, J = 1.5 Hz, 1H; Ar-CH), 8.46 (d, J = 1.5 Hz, 2H; Ar-CH), 10.52 (s, 1H; Ar-NH) ppm; ^{13}C{^{1}H} NMR (126 MHz, [D$_6$]DMSO, 25 °C, TMS): δ = 14.4 [S(CH$_3$)], 28.2 [C(CH$_3$)$_3$], 37.3, 40.0, 66.4, 69.1, 69.5, 69.67, 69.70, 69.73, 69.8 (CH$_2$ of PEG), 77.6 [C(CH$_3$)$_3$], 117.9, 118.7 (Ar-CH), 124.8 (Ar-C attached to C$_2$N$_2$O), 140.9 [Ar-C attached to NH(CO)PEG$_4$], 155.6 [PEG$_4$NH(CO)-OC(CH$_3$)$_3$], 164.2 (C$_2$N$_2$O attached to Ar), 165.4 [C$_2$N$_2$O attached to S(CH$_3$)], 170.2 [NH(CO)PEG$_4$NH(CO)OC-(CH$_3$)$_3$] ppm; HRMS (TOF): m/z calcd. for C$_{28}$H$_{40}$N$_6$O$_9$S$_2$+Na$^+$: 691.2217 [M+Na]$^+$; found: 691.2190.

*Synthesis of Compound **12**.* At 0 °C, *m*CPBA (114.8 mg, 0.670 mmol) was added slowly into a clear yellow solution of compound **11** (101.8 mg, 0.150 mmol) in dry DCM (4.0 mL). The reaction mixture stirred overnight at room temperature. It formed a clear colorless solution. The mixture was washed with 0.1 M aqueous solution of NaOH (6.0 mL). The organic phase was washed several times with deionized water until a neutral pH was achieved. The organic phase was dried over Na$_2$SO$_4$ and filtered before removing all volatiles under reduced pressure. Compound **12** was obtained as a glassy colorless solid (79.9 mg, 73% yield). ^{1}H NMR (500 MHz, [D$_6$]DMSO, 25 °C, TMS): δ = 1.36 [s, 9H; C(CH$_3$)$_3$], 2.65 (t, J = 6.0 Hz, 2H; CH$_2$ of PEG), 3.03 (q, J = 6.0 Hz, 2H; CH$_2$ of PEG), 3.30 (s, 3H; SO$_2$CH$_3$), 3.31−3.37 (m, 1H; CH$_2$ of PEG), 3.43−3.56 (m, 13H; CH$_2$ of PEG), 3.74 (s, 3H; SO$_2$CH$_3$), 3.75 (m, 2H; CH$_2$ of PEG), 6.74 [t, J = 5.2 Hz, 1H; ArNH(CO)-PEG$_4$NHBoc], 8.34 (m, 1H; Ar-CH), 8.66 (m, 1H; Ar-CH), 8.68 (m, 1H; Ar-CH), 10.66 [m, 1H; ArNH(CO)-PEG$_4$NHBoc] ppm; note: ^{1}H NMR sample contained small amount of *m*CPBA with signals at 7.54, 7.70, 7.87−7.91, 13.34 ppm; ^{13}C{^{1}H} NMR (126 MHz, [D$_6$]DMSO, 25 °C, TMS): δ = 28.2 [C(CH$_3$)$_3$], 37.3 (CH$_2$ of PEG), 43.1 (SO$_2$CH$_3$), 54.9, 66.3, 69.1, 69.5, 69.68, 69.72, 69.8 (CH$_2$ of PEG), 77.6 [C(CH$_3$)$_3$], 119.6, 119.8 (d, Ar-CH, J = 32.0 Hz), 120.5, 120.7 (d, Ar-CH, J = 32.0 Hz), 124.20 (Ar-C attached to C$_2$N$_2$O), 124.5 (Ar-CH), 141.2 (Ar-C attached to NH(CO)-PEG$_4$NHBoc), 155.6 [ArNH(CO)PEG$_4$NH(CO)OC-(CH$_3$)$_3$], 162.4 (C$_2$N$_2$O attached to Ar), 164.7, 164.8 (d, C$_2$N$_2$O attached to SO$_2$CH$_3$, J = 7.0 Hz), 164.9, 165.0 (d, C$_2$N$_2$O attached to SO$_2$CH$_3$, J = 6.0 Hz), 170.4 [ArNH-(CO)PEG$_4$NH(CO)OC(CH$_3$)$_3$] ppm; note: ^{13}C NMR sample contained small amount of *m*CPBA with signals at 120.2, 127.9, 128.8, 130.7, 167.7 ppm; ^{13}C NMR sample contained small amount of *m*CPBA with signals at 127.9, 128.8, 130.7, 167.7 ppm; HRMS (TOF): m/z calcd. for C$_{28}$H$_{40}$N$_6$O$_{13}$S$_2$+Na$^+$: 755.1960 [M+Na]$^+$; found: 755.1987.

Synthesis of DiPODS. Compound **12** (64.9 mg, 0.089 mmol) was dissolved in a 1:1 mixture of TFA:DCM (6 mL). It was stirred for 3 h at room temperature to facilitate Boc deprotection. The reaction solvent was removed under reduced pressure while the majority of TFA was removed azeotropically by washing the reaction mixture several times with toluene. The crude product was dissolved in deionized water (7.0 mL) and EtOAc (4.0 mL). The aqueous phase was washed two times with EtOAc (2 × 4.0 mL). The aqueous phase was freeze−dried for 24 h to afford DiPODS as a fine, off-white solid (50.6 mg, 90%). ^{1}H NMR (500 MHz, [D$_6$]DMSO, 25 °C, TMS): δ = 2.65 (t, J = 6.0 Hz, 2H; CH$_2$ of PEG), 2.96 (q, J = 5.2 Hz, 2H; CH$_2$ of PEG), 3.27−3.31 (m, 1H; CH$_2$ of PEG), 3.30 (s, 3H; SO$_2$CH$_3$), 3.46−3.58 (m, 14H; CH$_2$ of PEG), 3.75 (s, 3H; SO$_2$CH$_3$), 3.73−3.77 (m, 1H; CH$_2$ of PEG), 7.72 (br, 2H; ArNH(CO)PEG$_4$NHBoc), 8.34 (m, 1H; Ar-CH), 8.66 (m, 1H; Ar-CH), 8.68 (m, 1H; Ar-CH), 10.68 (m, 1H; ArNH(CO)PEG$_4$NH$_2$) ppm; ^{13}C{^{1}H} NMR (126 MHz, [D$_6$]DMSO, 25 °C, TMS): δ = 27.4, 37.3, 38.6 (CH$_2$ of PEG), 43.1 (SO$_2$CH$_3$), 56.0, 66.3, 66.7, 69.59, 69.66, 69.69, 69.73 (CH$_2$ of PEG), 119.6, 119.8 (d, Ar-CH, J = 32.5 Hz), 120.5, 120.7 (d, Ar-CH, J = 32.5 Hz), 124.2 (Ar-CH), 124.5 (Ar-C attached to C$_2$N$_2$O), 140.9, 141.2 [d, Ar-C

https://dx.doi.org/10.1021/acs.bioconjchem.0c00590
Bioconjugate Chem. 2020, 31, 2789−2806

attached to NH(CO)PEG$_4$NH$_2$, J = 27.0 Hz], 162.4 ($\underline{C}_2N_2O$ attached to Ar), 164.7 ($\underline{C}_2N_2O$ attached to SO_2CH_3), 170.4 [ArNH($\underline{C}$O)PEG$_4$NH$_2$] ppm; note: ^{13}C NMR sample contained small amount of *m*CPBA with signals at 127.9, 128.8, 130.7, 132.7, 166.1, 167.8 ppm; HRMS (TOF): m/z calcd. for $C_{23}H_{32}N_6O_{11}S_2$+H$^+$: 633.1646 [M+H]$^+$; found: 633.1643.

Synthesis of DiPODS-FITC. Diisopropylethylamine (0.11 mL, 0.63 mmol) was added into a clear colorless solution of DiPODS (72.0 mg, 0.114 mmol) in dry DMF (7.0 mL). This solution was stirred for 10 min before adding it dropwise into a solution of dye (48.6 mg, 0.125 mmol) in dry DMF (1.3 mL). The reaction vessel was covered with aluminum foil and it was stirred overnight at room temperature. All volatiles were removed under high vacuum. The obtained orange residue was redissolved in 40% MeCN and water (46.0 mL) for semipreparative RP-HPLC purification. The product, DiPODS-FITC, was obtained as an orange fluffy solid (50.9 mg, 44%). ^{1}H NMR (500 MHz, [D$_6$]DMSO, 25 °C, TMS): δ = 2.63 (t, J = 6.4 Hz, 2H; C$\underline{H}_2$ of PEG), 3.29 (s, 6H; $SO_2C\underline{H}_3$), 3.48−3.54 (12H; C$\underline{H}_2$ of PEG), 3.56 (m, 2H; C$\underline{H}_2$ of PEG), 3.65 (br, 2H; C$\underline{H}_2$ of PEG), 3.73 (t, J = 6.4 Hz, 2H; C$\underline{H}_2$ of PEG), 6.48−6.66 (br, 8H; from FITC dye), 7.14 (d, J = 8.5 Hz, 1H; FL-dye), 7.72 [br, 1H; ArNH(CO)PEG$_4$N$\underline{H}$-(CS)NH attached to FL-dye], 8.23 (br, 2H; O$\underline{H}$ of FL-dye), 8.32 (t, J = 1.4 Hz, 1H; Ar-C$\underline{H}$), 8.65 (d, J = 1.4 Hz, 2H; Ar-C$\underline{H}$), 10.18 [s, 1H; ArNH(CO)PEG$_4$NH(CS)N$\underline{H}$ attached to FL-dye], 10.76 [s, 1H; ArN$\underline{H}$(CO)PEG$_4$NH(CS)NH attached to FL-dye] ppm; ^{13}C{^{1}H} NMR (126 MHz, [D$_6$]DMSO, 25 °C, TMS): δ = 20.7, 37.3, 42.6 ($\underline{C}H_2$ of PEG), 43.7 ($SO_2\underline{C}H_3$), 66.4, 68.4, 69.6−69.8 ($\underline{C}H_2$ of PEG), 102.1 (Ar-$\underline{C}$H of FL-dye), 102.3 (Ar-$\underline{C}$H of FL-dye), 119.3 (Ar-$\underline{C}$H of FL-dye), 120.2 (Ar-$\underline{C}$H of FL-dye), 124.4 (Ar-$\underline{C}$ of DiPODS attached to C_2N_2O), 129.2 (Ar-$\underline{C}$H of FL-dye) and (Ar-$\underline{C}$ of FL-dye), 141.2 (Ar-$\underline{C}$ of FL-dye) and [Ar-$\underline{C}$ attached to NH(CO)PEG$_4$NH-FL-dye], 152.4 (Ar-$\underline{C}$ of FL-dye), 165.0 ($\underline{C}_2N_2O$ attached to Ar), 167.7 ($\underline{C}_2N_2O$ attached to SO_2CH_3), 168.6 ($\underline{C}$O of FL-dye), 170.4 [ArNH($\underline{C}$O)PEG$_4$NH-FL-dye], 180.5 [ArNH(CO)PEG$_4$NH($\underline{C}$S)NH attached to FL-dye] ppm; HRMS (TOF): m/z calcd. for $C_{44}H_{43}N_7O_{16}S_3$-2O +Na$^+$: 1012.1951 [M-2O+Na]$^+$; found: 1012.1914.

Variable Temperature NMR Experiments. Two NMR samples were prepared in [D$_6$]DMSO in 5 mm Wilmad High Throughput borosilicate NMR tubes. As described above, compound **1** contained a mixture of components, which were partially separated by successive precipitations out of cold DCM. The crude compound **1** mixture was separated into (1) solid precipitate containing set **A** (anti-rotamers), and (2) the components remaining in the mother liquor, which were dried under vacuum. The first NMR sample contained 5.21 mg of the residue isolated from the mother liquor, which was composed of a mixture of set **A** (*anti*-rotamers of compound **1**, *anti*-**1**), set **B** [doubly Boc-protected derivative of compound **1**, (Boc)$_2$-**1**], and set **C** (tautomers of compound **1**, tautomer-**1**). The second NMR sample contained the precipitate, *anti*-rotamers of compound **1** (set **A**, *anti*-**1**) (5.21 mg, 00168 mmol). Both samples were dissolved in [D$_6$]DMSO (0.41 and 0.40 mL, respectively) immediately before subjecting them to ^{1}H NMR analysis at 25 °C (298.15 K) on a Bruker Avance III HD 600 MHz spectrometer, with 16 scans collected every 10 min for 1 h. Once the scans were completed at 25 °C (298.15 K), the temperature was increased to 75 °C (348.15 K) and stabilized for 10 min before re-tuning, re-shimming, and re-locking the system onto the deuterated solvent signal for the acquisition of 16 scans every 10 min for 1 h. This process was repeated for each sample at 80 °C (353.15 K), 85 °C (358.15 K), and 90 °C (363.15 K). Calculations implementing the experimental data were based on the integrated values of the peaks located in the designated regions of the ^{1}H NMR spectra. The integration values of peaks located at 8.09 (t, J = 1.4 Hz, 1H; Ar-C$\underline{H}$), 8.41 (t, J = 1.4 Hz, 1H; Ar-C$\underline{H}$), and 8.45 (t, J = 2.9 Hz, 1H; Ar-C$\underline{H}$) ppm were used for assessing the proportions of set **A** (*anti*-rotamers of compound **1**, *anti*-**1**), set **B** [doubly Boc-protected derivative of compound **1**, (Boc)$_2$-**1**], and set **C** (imidic acid tautomer of compound **1**, tautomer-**1**), respectively. Integration values of peaks located at 7.88 (t, J = 1.5 Hz, 1H; Ar-C$\underline{H}$), 8.10 (t, J = 1.5 Hz, 1H; Ar-C$\underline{H}$), 8.14 (t, J = 1.5 Hz, 1H; Ar-C$\underline{H}$), 8.42 (t, J = 1.5 Hz, 1H; Ar-C$\underline{H}$), and 8.46 (t, J = 2.8 Hz, 1H; Ar-C$\underline{H}$) ppm were used for assessing the proportions of the Boc-deprotected derivative of compound **1**, set **A** (*anti*-rotamers of compound **1**, *anti*-**1**), set **D** (*syn*-rotamers of compound **1**, *syn*-**1**), set **B** [doubly Boc-protected derivative of compound **1**, (Boc)$_2$-**1**], and set **C** (tautomer of compound **1**, tautomer-**1**), respectively. The data acquired from these experiments are summarized in Table S1.

The first contained only the precipitate—i.e., the *anti*-rotamers (Figure 2C, set **A**). The second contained the mixture isolated from the mother liquor following precipitation (Figure 2D). The latter is composed mostly of the compounds responsible for sets **B** and **C** but also some of the *anti*-rotamer (set **A**). While the initial ^{1}H NMR of the sample of the *anti*-rotamers displayed only the peaks of set **A**, that of the mother liquor mixture showed the peaks of sets **A**, **B**, and **C** in a ratio of 1.0:1.5:1.6, respectively. The ^{1}H NMR spectra for both samples were collected again after 24 h at room temperature where no new peaks were observed in either sample and no change in the ratio between the peaks was observed in the spectrum of the mother liquor mixture.

Subsequently, variable temperature ^{1}H NMR spectra of the sample containing the mother liquor mixture were collected every 10 min for 1 h at 25, 75, 80, 85, and 90 °C. Upon heating the mother liquor mixture sample to 90 °C, the proportion of peaks from set **A** increased, while those of sets **B** and **C** decreased (Figure 2E, Table S1). Indeed, the proportion of the peaks in set **C** shrank to nearly zero (Table S1 and Figures S35 and S36). We also observed the appearance of two new sets of peaks in the sample at this elevated temperature. The first new set—set **D**—contained signals for all of the functional groups of compound **1** and was assigned to the *syn*-rotamers. The second new set was assigned to the Boc-deprotected variant of compound **1**. Importantly, however, the signals of set **D** were not significant, suggesting that sets **B** and **C** were converted to set **A** at the elevated temperature (Table S1).

Computational Studies. All calculations were performed with the Gaussian 16 software package revision B.01.[37] The B3LYP exchange-correlation functional with the polarized diffuse split-valence 6-311+G(d,p) basis set was used for all geometry optimizations, transition state calculations, and infrared frequency calculations. For calculating solvent effects, the integral equation formalism model (IEFPCM)[40] (DMSO) was used.[41] For the molecular cavities, the united atom topological model for Hartree−Fock (UAHF) was used.[42] Before performing calculations at a high level of theory with the Gaussian 16 software, two calculations were performed for each compound using the Spartan 14 software package. First, a large set of conformers were generated using the Merck

https://dx.doi.org/10.1021/acs.bioconjchem.0c00590
Bioconjugate Chem. 2020, 31, 2789−2806

Molecular Force Fields (MMFF). Then, structures with the lowest energies (within 3.0 kcal/mol energy difference) were optimized at the HF/3-21G level of theory. Then, the lowest energy conformers (within 3 kcal/mol energy difference) were submitted to Gaussian 16 for full optimization at the level of theory described above. The frequency calculations were used to evaluate conformers' zero-point vibrational energy (ZPVE) and thermal corrections at 298.15 K. For all ground-state conformers, all harmonic vibrational frequencies were positive, confirming that they were local minima. For thermodynamic evaluation of ethanethiol conjugations, all reactions were computed with UAHF for improved solvent modeling, and all reactions were performed as isodesmic, so total energy differences could be compared. For P2, the most stable optimized geometry from a separate geometry optimization calculation without UAHF was used in a single point energy calculation with UAHF. All graphical depictions of the structures were generated using CYLview software[43] using coordinates from the optimized log file.

Bioconjugation. *Preparation of Reduced Fab_{HER2}.* To a suspension of 150 μg of Fab_{HER2} in PBS pH 7.4 (1.19 mg/mL) was added the appropriate volume of a fresh TCEP solution (10 mM in water) to reduce the interchain disulfide bridge. The reaction mixture was stirred on a thermomixer (25 or 37 °C) for 2 h. The reductant was then removed using centrifugal filtration units with a 3000 Da molecular weight cut off (Amicon Ultra 0.5 Centrifugal Filtration Units, Millipore Corp. Billerica, MA) at 4 °C with fresh PBS pH = 7.4. The reaction mixture was immediately stored at 4 °C.

Preparation of Reduced Fab_{ns}. To a suspension of 150 μg of Fab_{ns} in PBS pH 7.4 (14.64 mg/mL) was added 5.99 μL of a fresh TCEP solution (10 mM in water). The reaction mixture was stirred on a thermomixer (25 or 37 °C) for 2 h. The reductant was then removed using centrifugal filtration units with a 3000 Da molecular weight cutoff (Amicon Ultra 0.5 Centrifugal Filtration Units, Millipore Corp. Billerica, MA) at 4 °C with fresh PBS pH = 7.4. The reaction mixture was immediately stored at 4 °C.

Preparation of Fab_{HER2}-DiPODS-FITC. To a suspension of 150 μg of Fab_{HER2} in PBS pH 7.4 (1.19 mg/mL) was added 5.99 μL of a fresh TCEP solution (10 mM in water, 20 equiv). The reaction mixture was stirred on a thermomixer (37 °C) for 2 h. The reductant was then removed using centrifugal filtration units with a 3000 Da molecular weight cutoff (AmiconTM Ultra 0.5 Centrifugal Filtration Units, Millipore Corp. Billerica, MA) at 4 °C with fresh PBS pH = 7.4. The appropriate volume of a DiPODS-FITC solution (10 mM in DMSO) was immediately added to the reduced Fab_{HER2}. The reaction mixture was stirred on a thermomixer at 37 °C for 16 h. The conjugate was then purified on a size exclusion column (Sephadex G-25 M, PD-10 column, GE Healthcare; dead volume = 2.5 mL, eluted with 2 mL of PBS, pH 7.4) and concentrated using centrifugal filtration units with a 30 000 Da molecular weight cutoff (Amicon Ultra 0.5 Centrifugal Filtration Units, Millipore Corp. Billerica, MA).

Preparation of Fab_{ns}-DiPODS-FITC. To a suspension of 150 μg of Fab_{ns} in PBS pH 7.4 (14.64 mg/mL) was added 5.99 μL of a fresh TCEP solution (10 mM in water, 20 equiv).The reaction mixture was stirred on a thermomixer (37 °C) for 2 h. The reductant was then removed using centrifugal filtration units with a 3000 Da molecular weight cutoff (AmiconTM Ultra 0.5 Centrifugal Filtration Units, Millipore Corp. Billerica, MA) at 4 °C with fresh PBS pH = 7.4. The appropriate volume of a DiPODS-FITC solution (10 mM in DMSO) was immediately added to the reduced Fab_{ns}. The reaction mixture was stirred on a thermomixer at 37 °C for 16 h. The conjugate was then purified on a size exclusion column (Sephadex G-25 M, PD-10 column, GE Healthcare; dead volume = 2.5 mL, eluted with 2 mL of PBS, pH 7.4) and concentrated using centrifugal filtration units with a 30 000 Da molecular weight cutoff (Amicon Ultra 0.5 Centrifugal Filtration Units, Millipore Corp. Billerica, MA).

Preparation of Fab_{HER2}-Lys-FITC Conjugate. Bioconjugation conditions were adjusted in order to obtain a DOL of ~1 for the final conjugate. To a suspension of 150 μg of Fab_{HER2} in PBS pH 7.4 (1.19 mg/mL) was added 12.5 μL of a fresh Na_2CO_3 solution (0.1 mM in water) to adjust the pH to 9.0. 1.13 μL of an NCS-FITC solution (10 mM in DMSO, 3.75 equiv) were then added. The reaction mixture was stirred on a thermomixer at 37 °C for 1 h. The conjugate was then purified on a size exclusion column (Sephadex G-25 M, PD-10 column, GE Healthcare; dead volume = 2.5 mL, eluted with 2 mL of PBS, pH 7.4) and concentrated using centrifugal filtration units with a 30 000 Da molecular weight cutoff (Amicon Ultra 0.5 Centrifugal Filtration Units, Millipore Corp. Billerica, MA).

Biological Characterization. *Procedure for Quantitating Fluorescein Degree of Labeling.* UV−vis measurements were taken on a Shimadzu BioSpec-Nano Micro-Volume UV−vis Spectrophotometer (Shimadzu, Kyoto, Japan). The fluorescein to Fab ratio was determined via UV−vis spectrophotometry of the conjugates at 280 and 495 nm followed by calculation using the following equation:

$$\mathrm{Abs_{Fab}} = \mathrm{Abs_{280}} - (\mathrm{Abs_{495}} \times \mathrm{CF})$$

$$\mathrm{DOL} = [\mathrm{Abs_{max}} \times \mathrm{MW_{Fab}}]/[[\mathrm{Fab}] \times \varepsilon\mathrm{Dye_{495}}]$$

in which the correction factor (CF) for DiPODS-FITC was 0.34 based on the absorbance spectrum of DiPODS-FITC in PBS, $\mathrm{MW_{Fab}}$ = 50 000, $\varepsilon\mathrm{Dye_{495}}$ = 75 000, and ε_{280}, mAb = 69 000.

Procedure for Quantitating Sulfhydryl Groups. To a suspension of 150 μg of Fab in PBS pH 7.4 was added 50 μL of a fresh solution of the Ellman's reagent[44] (10 mM in DMSO/water, 25% v/v) and the appropriate volume of PBS to obtain a final volume of reaction mixture of 250 μL. The reaction mixture was stirred on a thermomixer protected from light for 30 min. The sulfhydryl to Fab ratio was determined via UV−vis spectrophotometry of the Fab mixture at 412 nm followed by calculation using the following equation:

$$\mathrm{Ratio{-}SH/Fab} = \{[(\mathrm{Abs_{412}}/\varepsilon\mathrm{DTNB_{412}}) \times V_{\mathrm{reaction}}]/V_{\mathrm{Fab}}\} \times 10^6/[\mathrm{Fab}]$$

in which $\varepsilon\mathrm{DTNB_{412}}$ = 14 150 $\mathrm{M^{-1}cm^{-1}}$, V_{reaction} (L) = 250 (μL) × 10^{-6}, and V_{Fab} is the volume for 150 μg of Fab in liters.

SDS-PAGE Analysis of Conjugates. 5 μg of Fab (5 μL of a 1.0 mg/mL stock) was combined with 18.5 μL H_2O, and 7.5 μL 4× electrophoresis buffer (NuPAGE LDS Sample Buffer, Thermo Fisher, Eugene, OR). This mixture was then denatured by heating to 60 °C for 5 min using an agitating thermomixer. Subsequently, 20 μL of each sample was then loaded alongside an appropriate molecular weight marker (Novex Sharp Pre- Stained Protein Ladder, Life Technologies) onto a 1 mm, 10 well 4−12% Bis-Tris protein gel (Life Technologies) and run for ~4 h at 80 V in MOPS buffer. The completed gel was washed 3 times with H_2O, stained using

https://dx.doi.org/10.1021/acs.bioconjchem.0c00590
Bioconjugate Chem. 2020, 31, 2789−2806

SimplyBlueTM SafeStain (Life Technologies) for 1 h, and then destained overnight in H_2O. The gel was then analyzed using an Odyssey CLx Imaging system (LI-COR Biosciences, Lincoln, NE). Fluorescence signal was analyzed using a Typhoon FLA 7000 Imaging system (GE Healthcare, USA).

Analytical Size-Exclusion Chromatography. Analytical size-exclusion chromatography (A-SEC) of the Fab_{HER2}-DiPODS-FITC was conducted on a Shimadzu UFLC System with a SPD-20A UV−vis Detector, CBM-20A system controller, DGU-20A3R degassing unit, and LC-20AB binary pump using a Superdex 200 Increase 10/300 GL column (GE Healthcare, USA) with a flow rate of 0.75 mL/min. Elution of conjugates have been achieved during a 45 min isocratic gradient using a phosphate buffer at pH 7.4 as a mobile phase. UV chromatograms were recorded at 280 nm.

Stability Study in Human Serum Albumin. In an Eppendorf tube, 150 μL human serum albumin (HSA) were mixed with 50 μL Fab_{HER2}-DiPODS-FITC (2.0 mg/mL) for each sample individually to give a final solution of 0.5 mg/mL conjugates in 75% HSA serum. Samples were incubated at 37 °C for 1, 2, 3, 4, 5, 6, and 7 days. Samples (50 μL) were quenched with an extraction buffer (100 μL) consisting of 50% ACN/H_2O, 0.1 M NaCl, and 1% TFA, chilled on ice for 5 min, centrifuged (14 000 rpm, 10 min) and analyzed (2 × 25 μL injection) by SEC-HPLC. Samples were prepared and analyzed in triplicate.

MALDI-ToF Mass Spectrometry. As a means by which to quantify the number of cargoes per antibody, the Fab conjugates were analyzed by MALDI-ToF MS/MS using a Bruker Ultraflex MALDI-ToF/ToF (Bruker Daltonic GmbH). 1 μL of each sample (1 mg/mL) was mixed with 1 μL of sinapic acid (10 mg/mL in 50% acetonitrile:water and 0.1% trifluoroacetic acid). 1 μL of the sample/matrix solution was spotted onto a stainless steel target plate and allowed to air-dry. All mass spectra were obtained using a Bruker Ultraflex MALDI-ToF/ToF (Bruker Daltonic GmbH). Ions were analyzed in positive mode and external calibration was performed by use of a standard protein mixture (Bovine Serum Albumin). Samples were prepared and analyzed in triplicate.

The degree of labeling (DOL) of Fab_{HER2}-DiPODS-FITC was calculated from MALDI-ToF spectra analysis using the following equation:

$$\mathrm{DOL} = (m/z\ \mathrm{Fab_{HER2}{-}DiPODS{-}FITC} - m/z\ \mathrm{Fab_{HER2}}) / (m/z\ \mathrm{DiPODS{-}FITC})$$

in which m/z DiPODS−FITC is ∼927. After calculation, a DOL of ∼1 was obtained.

Circular Dichroism Spectroscopy. All circular dichroism (CD) spectroscopy was performed using a Chirascan V100 (Applied Photophysics Ltd., UK). Temperature was controlled via the Pro-Data Chirascan program and monitored with the Chirascan CS/PSM Turret T1 temperature probe. The far UV CD spectra of Fab_{HER2}, reduced Fab_{HER2}, and Fab_{HER2}-DiPODS-FITC (0.12 mg/mL in PBS Buffer, pH 7.4) were taken from 200 to 280 nm at 5 °C in 1 mm optical path quartz cuvettes. Spectra values were corrected by subtracting buffer baselines determined in the same cuvette, and the adjusted values were then converted to mean residue molar ellipticity (MRE).

Thermal stability experiments were performed by taking CD spectra from 200 to 280 nm at 0.5 °C increments from 5 to 80 °C with an equilibration time of 2 min at each temperature. The data were subsequently analyzed using SciDAVis software in which thermal unfolding transition profiles for each fragment were obtained using CD signals at 205 nm. To this end, MRE values were converted to fraction folded, plotted against temperature, and fitted to a Boltzmann (Sigmoidal) curve. The melting temperatures—i.e., the temperature at which the faction folded is 0.5—were then extrapolated from the curves.

***In Vitro* Evaluation.** *Flow Cytometry.* Flow cytometry experiments were performed with HER2-positive BT474 cells. Modified Fab conjugates—Fab_{HER2}-DiPODS-FITC and Fab_{HER2}-Lys-FITC—were incubated at 0.8 mg/mL in suspension with 10^6 cells/mL, for 30 min on ice. Cells were washed by pelleting and resuspension three times, and then analyzed on a BD LSR-II (BD Biosciences). Samples were prepared and analyzed in triplicate.

■ ASSOCIATED CONTENT

Supporting Information

The Supporting Information is available free of charge at https://pubs.acs.org/doi/10.1021/acs.bioconjchem.0c00590.

Additional NMR figures including variable temperature NMR data, bioconjugation characterization, in vitro stability, size-exclusion HPLC, MALDI-TOF MS, CD figures, and flow cytometry data (PDF)

■ AUTHOR INFORMATION

Corresponding Authors

Eric W. Price − *Department of Chemistry, University of Saskatchewan, Saskatoon, Saskatchewan S7N-5C9, Canada;* orcid.org/0000-0002-8619-1199; Phone: +1.306.966.4788; Email: eric.price@usask.ca; Fax: +1.306.966.4666

Brian M. Zeglis − *Department of Chemistry, Hunter College, City University of New York, New York, New York 10021, United States; Ph.D. Program in Chemistry, The Graduate Center of the City University of New York, New York, New York 10021, United States; Department of Radiology, Memorial Sloan Kettering Cancer Center, New York, New York 10065, United States;* orcid.org/0000-0002-9091-744X; Phone: 212-896-0443; Email: bz102@hunter.cuny.edu; Fax: 212-896-0484

Authors

Elaheh Khozeimeh Sarbisheh − *Department of Chemistry, University of Saskatchewan, Saskatoon, Saskatchewan S7N-5C9, Canada*

Guillaume Dewaele-Le Roi − *Department of Chemistry, Hunter College, City University of New York, New York, New York 10021, United States; Ph.D. Program in Chemistry, The Graduate Center of the City University of New York, New York, New York 10021, United States; Department of Radiology, Memorial Sloan Kettering Cancer Center, New York, New York 10065, United States*

Whitney E. Shannon − *Department of Chemistry, University of Saskatchewan, Saskatoon, Saskatchewan S7N-5C9, Canada*

Sally Tan − *Department of Chemistry, Hunter College, City University of New York, New York, New York 10021, United States*

https://dx.doi.org/10.1021/acs.bioconjchem.0c00590
Bioconjugate Chem. 2020, 31, 2789−2806

Yujia Xu − *Department of Chemistry, Hunter College, City University of New York, New York, New York 10021, United States; Ph.D. Program in Chemistry, The Graduate Center of the City University of New York, New York, New York 10021, United States*

Complete contact information is available at: https://pubs.acs.org/10.1021/acs.bioconjchem.0c00590

Author Contributions

[#]E.K.S. and G.D.-L. contributed equally to this work.

Notes

The authors declare no competing financial interest.

■ ACKNOWLEDGMENTS

The authors thank the National Institutes of Health (BMZ: R01CA240963, U01CA221046, R01CA204167, R21EB030275, and R01CA244327), the Tow Foundation (GDLR), the Natural Sciences and Engineering Research Council of Canada (EWP: RGPIN-2017-03952), the Canada Research Chairs program (EWP: Tier 2 CRC #231072), the Canadian Institutes of Health Research (CIHR Project Grant #388243), the Canadian Foundation for Innovation John Evans Leadership Fund (CRC-JELF, EWP: #35162), the Sylvia Fedoruk Canadian Centre for Nuclear Innovation (EWP: Project Grants), the Saskatchewan Health Research Foundation (EWP: Establishment Grant, EKS: PDF fellowship), and startup funds from the University of Saskatchewan Department of Chemistry and College of Arts and Sciences.

■ ABBREVIATIONS

ADC, antibody−drug conjugates; PODS, phenyloxadiazolyl methyl sulfone; VT-NMR, variable temperature nuclear magnetic resonance; HPLC, high-pressure liquid chromatography; FITC, fluorescein; Fab, fragment antigen binding; *m*CPBA, *meta*-chloroperoxybenzoic acid; PEG, polyethylene glycol; HATU, 1-[bis(dimethylamino)methylene]-1*H*-1,2,3-triazolo[4,5*b*]pyridinium 3-oxide; DIEA, *N*,*N*-diisopropylethylamine; TMP, 2,4,6-trimethylpyridine; EEDQ, *N*-ethoxycarbonyl-2-ethoxy-1,2-dihydroquinoline; EDC, 1-ethyl-3-(3-(dimethylamino)propyl)carbodiimide; DCM, dichloromethane; DFT, density functional theory

■ REFERENCES

(1) Legault, C. Y. *CYLView, 1.0b*; Université de Sherbrooke, Canada, 2009−2012, http://www.cylview.org.

(2) *Radiopharmaceutical Chemistry*, 1 ed., Springer International Publishing, Springer Nature Switzerland AG, 2019.

(3) Adumeau, P., Davydova, M., and Zeglis, B. M. (2018) Thiol-Reactive Bifunctional Chelators for the Creation of Site-Selectively Modified Radioimmunoconjugates with Improved Stability. *Bioconjugate Chem. 29*, 1364−1372.

(4) Dozier, J. K., and Distefano, M. D. (2015) Site-Specific PEGylation of Therapeutic Proteins. *Int. J. Mol. Sci. 16*, 25831−64.

(5) Freidel, C., Kaloyanova, S., and Peneva, K. (2016) Chemical tags for site-specific fluorescent labeling of biomolecules. *Amino Acids 48*, 1357−72.

(6) Behrens, C. R., and Liu, B. (2014) Methods for site-specific drug conjugation to antibodies. *mAbs 6*, 46−53.

(7) Adumeau, P., Vivier, D., Sharma, S. K., Wang, J., Zhang, T., Chen, A., Agnew, B. J., and Zeglis, B. M. (2018) Site-Specifically Labeled Antibody-Drug Conjugate for Simultaneous Therapy and ImmunoPET. *Mol. Pharmaceutics 15*, 892−898.

(8) Adumeau, P., Sharma, S. K., Brent, C., and Zeglis, B. M. (2016) Site-Specifically Labeled Immunoconjugates for Molecular Imaging–Part 1: Cysteine Residues and Glycans. *Mol. Imaging Biol. 18*, 1−17.

(9) Renault, K., Fredy, J. W., Renard, P. Y., and Sabot, C. (2018) Covalent Modification of Biomolecules through Maleimide-Based Labeling Strategies. *Bioconjugate Chem. 29*, 2497−2513.

(10) Beck, A., Goetsch, L., Dumontet, C., and Corvaia, N. (2017) Strategies and challenges for the next generation of antibody-drug conjugates. *Nat. Rev. Drug Discovery 16*, 315−337.

(11) Alley, S. C., Benjamin, D. R., Jeffrey, S. C., Okeley, N. M., Meyer, D. L., Sanderson, R. J., and Senter, P. D. (2008) Contribution of Linker Stability to the Activities of Anticancer Immunoconjugates. *Bioconjugate Chem. 19*, 759−765.

(12) Baldwin, A. D., and Kiick, K. L. (2011) Tunable degradation of maleimide-thiol adducts in reducing environments. *Bioconjugate Chem. 22*, 1946−53.

(13) Jackson, D., Atkinson, J., Guevara, C. I., Zhang, C., Kery, V., Moon, S. J., Virata, C., Yang, P., Lowe, C., Pinkstaff, J., et al. (2014) In vitro and in vivo evaluation of cysteine and site specific conjugated herceptin antibody-drug conjugates. *PLoS One 9*, e83865.

(14) Ponte, J. F., Sun, X., Yoder, N. C., Fishkin, N., Laleau, R., Coccia, J., Lanieri, L., Bogalhas, M., Wang, L., Wilhelm, S., et al. (2016) Understanding How the Stability of the Thiol-Maleimide Linkage Impacts the Pharmacokinetics of Lysine-Linked Antibody-Maytansinoid Conjugates. *Bioconjugate Chem. 27*, 1588−1598.

(15) Shen, B. Q., Xu, K., Liu, L., Raab, H., Bhakta, S., Kenrick, M., Parsons-Reponte, K. L., Tien, J., Yu, S. F., Mai, E., et al. (2012) Conjugation site modulates the in vivo stability and therapeutic activity of antibody-drug conjugates. *Nat. Biotechnol. 30*, 184−189.

(16) Toda, N., Asano, S., and Barbas, C. F., 3rd. (2013) Rapid, stable, chemoselective labeling of thiols with Julia-Kocienski-like reagents: a serum-stable alternative to maleimide-based protein conjugation. *Angew. Chem., Int. Ed. 52*, 12592−12596.

(17) Patterson, J. T., Asano, S., Li, X., Rader, C., and Barbas, C. F., 3rd. (2014) Improving the serum stability of site-specific antibody conjugates with sulfone linkers. *Bioconjugate Chem. 25*, 1402−1407.

(18) Davydova, M., Dewaele Le Roi, G., Adumeau, P., and Zeglis, B. M. (2019) Synthesis and Bioconjugation of Thiol-Reactive Reagents for the Creation of Site-Selectively Modified Immunoconjugates. *J. Visualized Exp. 145*, e59063.

(19) Li, X., Patterson, J. T., Sarkar, M., Pedzisa, L., Kodadek, T., Roush, W. R., and Rader, C. (2015) Site-Specific Dual Antibody Conjugation via Engineered Cysteine and Selenocysteine Residues. *Bioconjugate Chem. 26*, 2243−2248.

(20) Badescu, G., Bryant, P., Bird, M., Henseleit, K., Swierkosz, J., Parekh, V., Tommasi, R., Pawlisz, E., Jurlewicz, K., Farys, M., et al. (2014) Bridging disulfides for stable and defined antibody drug conjugates. *Bioconjugate Chem. 25*, 1124−1136.

(21) Schumacher, F. F., Sanchania, V. A., Berend Tolner, B., Wright, Z. V. F., Ryan, C. P., Smith, M. E. B., Ward, J. M., Caddick, S., M, K. C. W., Aeppli, G., et al. (2013) Homogeneous antibody fragment conjugation by disulfide bridging introduces 'spinostics. *Sci. Rep. 3*, 1525.

(22) Bryden, F., Maruani, A., Savoie, H., Chudasama, V., Smith, M. E., Caddick, S., and Boyle, R. W. (2014) Regioselective and stoichiometrically controlled conjugation of photodynamic sensitizers to a HER2 targeting antibody fragment. *Bioconjugate Chem. 25*, 611−617.

(23) Wang, T., Riegger, A., Lamla, M., Wiese, S., Oeckl, P., Otto, M., Wu, Y., Fischer, S., Barth, H., Kuan, S. L., et al. (2016) Water-soluble allyl sulfones for dual site-specific labelling of proteins and cyclic peptides. *Chem. Sci. 7*, 3234−3239.

(24) Kuan, S. L., Wang, T., and Weil, T. (2016) Site-Selective Disulfide Modification of Proteins: Expanding Diversity beyond the Proteome. *Chem. - Eur. J. 22*, 17112−17129.

(25) Schumacher, F. F., Nunes, J. P., Maruani, A., Chudasama, V., Smith, M. E., Chester, K. A., Baker, J. R., and Caddick, S. (2014) Next generation maleimides enable the controlled assembly of antibody-

drug conjugates via native disulfide bond bridging. *Org. Biomol. Chem. 12*, 7261−9.
(26) Nunes, J. P., Morais, M., Vassileva, V., Robinson, E., Rajkumar, V. S., Smith, M. E., Pedley, R. B., Caddick, S., Baker, J. R., and Chudasama, V. (2015) Functional native disulfide bridging enables delivery of a potent, stable and targeted antibody-drug conjugate (ADC). *Chem. Commun. (Cambridge, U. K.) 51*, 10624−7.
(27) Smith, M. E. B., Schumacher, F. F., Ryan, C. P., Tedaldi, L. M., Papaioannou, D., Waksman, G., Caddick, S., and Baker, J. R. (2010) Protein Modification, Bioconjugation, and Disulfide Bridging Using Bromomaleimides. *J. Am. Chem. Soc. 132*, 1960−1965.
(28) Behrens, C. R., Ha, E. H., Chinn, L. L., Bowers, S., Probst, G., Fitch-Bruhns, M., Monteon, J., Valdiosera, A., Bermudez, A., Liao-Chan, S., et al. (2015) Antibody-Drug Conjugates (ADCs) Derived from Interchain Cysteine Cross-Linking Demonstrate Improved Homogeneity and Other Pharmacological Properties over Conventional Heterogeneous ADCs. *Mol. Pharmaceutics 12*, 3986−98.
(29) Morais, M., Nunes, J. P. M., Karu, K., Forte, N., Benni, I., Smith, M. E. B., Caddick, S., Chudasama, V., and Baker, J. R. (2017) Optimisation of the dibromomaleimide (DBM) platform for native antibody conjugation by accelerated post-conjugation hydrolysis. *Org. Biomol. Chem. 15*, 2947−2952.
(30) Maruani, A., Smith, M. E., Miranda, E., Chester, K. A., Chudasama, V., and Caddick, S. (2015) A plug-and-play approach to antibody-based therapeutics via a chemoselective dual click strategy. *Nat. Commun. 6*, 6645.
(31) Chudasama, V., Smith, M. E., Schumacher, F. F., Papaioannou, D., Waksman, G., Baker, J. R., and Caddick, S. (2011) Bromopyridazinedione-mediated protein and peptide bioconjugation. *Chem. Commun. (Cambridge, U. K.) 47*, 8781−3.
(32) Lee, M. T. W., Maruani, A., Baker, J. R., Caddick, S., and Chudasama, V. (2016) Next-generation disulfide stapling: reduction and functional re-bridging all in one. *Chem. Sci. 7*, 799−802.
(33) Walsh, S. J., Omarjee, S., Galloway, W., Kwan, T. T., Sore, H. F., Parker, J. S., Hyvonen, M., Carroll, J. S., and Spring, D. R. (2019) A general approach for the site-selective modification of native proteins, enabling the generation of stable and functional antibody-drug conjugates. *Chem. Sci. 10*, 694−700.
(34) Ohta, Y., Kamijyo, Y., Fujii, S., Yokoyama, A., and Yokozawa, T. (2011) Synthesis and Properties of a Variety of Well-Defined HyperbranchedN-Alkyl andN-H Polyamides by Chain-Growth Condensation Polymerization of AB2Monomers. *Macromolecules 44*, 5112−5122.
(35) Moraczewski, A. L., Banaszynski, L. A., From, A. M., White, C. E., and Smith, B. D. (1998) Using Hydrogen Bonding to Control Carbamate C-N Rotamer Equilibria. *J. Org. Chem. 63*, 7258−7262.
(36) Marcovici-Mizrahi, D., Gottlieb, H. E., Marks, V., and Nudelman, A. (1996) On the Stabilization of the Syn-Rotamer of Amino Acid Carbamate Derivatives by Hydrogen Bonding. *J. Org. Chem. 61*, 8402−8406.
(37) Frisch, M. J., Schlegel, H. B., Scuseria, G. E., Robb, M. A., Cheeseman, J. R., Scalmani, G., Barone, V., Mennucci, B., and Petersson, G. A.et al. (2010) *Gaussian 09*, Revision C.01., Gaussian, Inc., Wallingford, CT.
(38) Fulmer, G. R., Miller, A. J. M., Sherden, N. H., Gottlieb, H. E., Nudelman, A., Stoltz, B. M., Bercaw, J. E., and Goldberg, K. I. (2010) NMR Chemical Shifts of Trace Impurities: Common Laboratory Solvents, Organics, and Gases in Deuterated Solvents Relevant to the Organometallic Chemist. *Organometallics 29*, 2176−2179.
(39) *NMR Solvent Data Chart*, Cambridge Isotope Laboratories, Inc., Tewksbury, MA, 2020.
(40) Scalmani, G., and Frisch, M. J. (2010) Continuous surface charge polarizable continuum models of solvation. I. General formalism. *J. Chem. Phys. 132*, 114110.
(41) Marenich, A. V., Cramer, C. J., and Truhlar, D. G. (2009) Universal Solvation Model Based on Solute Electron Density and on a Continuum Model of the Solvent Defined by the Bulk Dielectric Constant and Atomic Surface Tensions. *J. Phys. Chem. B 113*, 6378−6396.
(42) Barone, V., Cossi, M., and Tomasi, J. (1997) A new definition of cavities for the computation of solvation free energies by the polarizable continuum model. *J. Chem. Phys. 107*, 3210−3221.
(43) Legault, C. Y. (2009−2012) *CYLView, 1.0b*, Université de Sherbrooke, Canada, http://www.cylview.org.
(44) Thermo Scientific. Ellman's Reagent. 2011.

https://dx.doi.org/10.1021/acs.bioconjchem.0c00590
Bioconjugate Chem. 2020, 31, 2789−2806